Original Research

Genetic Deletion of IL (Interleukin)-19 Exacerbates Atherogenesis in *Il19*$^{-/-}$×*Ldlr*$^{-/-}$ Double Knockout Mice by Dysregulation of mRNA Stability Protein HuR (Human antigen R)

Mitali Ray, Khatuna Gabunia, Christine N. Vrakas, Allison B. Herman, Farah Kako, Sheri E. Kelemen, Laurel A. Grisanti, Michael V. Autieri

Objective—To test the hypothesis that loss of IL (interleukin)-19 exacerbates atherosclerosis.

Approach and Results—*Il19*$^{-/-}$ mice were crossed into *Ldlr*$^{-/-}$ (low-density lipoprotein receptor knock out) mice. Double knockout (dKO) mice had increased plaque burden in aortic arch and root compared with *Ldlr*$^{-/-}$ controls after 14 weeks of high-fat diet (HFD). dKO mice injected with 10 ng/g per day rmIL-19 had significantly less plaque compared with controls. qRT-PCR and Western blot analysis revealed dKO mice had increased systemic and intraplaque polarization of T cells and macrophages to proinflammatory T_h1 and M1 phenotypes, and also significantly increased TNF (tumor necrosis factor)-α expression in spleen and aortic arch compared with *Ldlr*$^{-/-}$ controls. Bone marrow transplantation suggests that immune cells participate in IL-19 protection. Bone marrow-derived macrophages and vascular smooth muscle cells isolated from dKO mice had a significantly greater expression of inflammatory cytokine mRNA and protein compared with controls. Spleen and aortic arch from dKO mice had significantly increased expression of the mRNA stability protein HuR (human antigen R). Bone marrow-derived macrophage and vascular smooth muscle cell isolated from dKO mice also had greater HuR abundance. HuR stabilizes proinflammatory transcripts by binding AU-rich elements in the 3′ untranslated region. Cytokine and HuR mRNA stability were increased in dKO bone marrow-derived macrophage and vascular smooth muscle cell, which was rescued by addition of IL-19 to these cells. IL-19–induced expression of miR133a, which targets and reduced HuR abundance; miR133a levels were lower in dKO mice compared with controls.

Conclusions—These data indicate that IL-19 is an atheroprotective cytokine which decreases the abundance of HuR, leading to reduced inflammatory mRNA stability. (***Arterioscler Thromb Vasc Biol*, 2018;38:00-00. DOI: 10.1161/ATVBAHA.118.310929.**)

Key Words: atherosclerosis ■ bone marrow ■ cytokines ■ endothelial cells ■ macrophages

Atherosclerosis and other vascular inflammatory diseases continue to be a significant health and socioeconomic problem in the Western and developing world.[1] Atherosclerosis is a lipid-driven, chronic vascular inflammatory disease driven and maintained by proinflammatory cytokines secreted by both immune and vascular cells, with most studies focusing on the role of proinflammatory cytokines in activation of macrophages, endothelial cells, and leukocyte subsets in this disease.[2,3] By comparison, a much smaller number of studies focus on the role of endogenous counter-regulatory mechanisms in atherogenesis and their effects on these same cells and impact on atherosclerosis. Potential protective effects of anti-inflammatory cytokines including T_h2 interleukins on resident vascular (endothelial cell and vascular smooth muscle cell [VSMC]) and inflammatory cells remain as a gap in our knowledge. Antiatherosclerotic interleukins that can target resident vascular cells, in addition to immune cells, have the potential to reduce localized inflammation of the vascular wall as well as polarize global immunity. Identification of such interleukins can lead to potential therapeutic targets.

We have reported a distinctive role for one such anti-inflammatory interleukin, IL (interleukin)-19, in vascular disease.[4–6] IL-19 is a member of an IL-10 subfamily which also includes IL-20, IL-22, and IL-24.[7,8] IL-19 has unique properties including expression as well as target cells outside of the immune system and NF-κB–independent effects.[9] Although expression of T_h2 cytokines in atherosclerotic plaque is rare, we previously reported that IL-19 is expressed in multiple cell types in atherosclerotic plaque in both humans and mice.[10] We also observed increased IL-19 in symptomatic patients compared with asymptomatic patients. Injection of recombinant IL-19 into atherosclerosis-prone *Ldlr*$^{-/-}$ (low-density

Received on: July 20, 2017; final version accepted on: April 5, 2018.

From the Department of Physiology, Independence Blue Cross Cardiovascular Research Center, Lewis Katz School of Medicine at Temple University, Philadelphia, PA (M.R., K.G., C.N.V., A.B.H., F.K., S.E.K., M.V.A.); and Department of Biomedical Sciences, University of Missouri, Columbia (L.A.G.).

The online-only Data Supplement is available with this article at http://atvb.ahajournals.org/lookup/suppl/doi:10.1161/ATVBAHA.118.310929/-/DC1.

Correspondence to Michael Autieri, PhD, Department of Physiology, Independence Blue Cross Cardiovascular Research Center, Temple University School of Medicine, Room 1050, MERB 3500 N Broad St, Philadelphia, PA 19140. E-mail mautieri@temple.edu

Nonstandard Abbreviations and Acronyms	
AREs	AU-rich elements
BMDM	bone marrow-derived macrophage
dKO	double knockout
HFD	high-fat diet
HuR	human antigen R
IL	interleukin
Ldlr	low-density lipoprotein receptor
RBPs	mRNA binding proteins
TNF-α	tumor necrosis factor-α
UTR	untranslated region
VSMC	vascular smooth muscle cell

lipoprotein receptor knock out) mice can reduce the severity of atherosclerosis,[10] as well as prevent expansion of existing plaque[11] by multiple effects on adaptive immunity, including polarization of T cells to T_h2 and macrophages to M2 phenotypes, respectively.

In response to proinflammatory stimuli, gene expression in resident vascular and immune cells is regulated by transcriptional and post-transcriptional mechanisms. Factors that control mRNA stability are essential regulators, which allow these cells to rapidly and appropriately respond to environmental cues. The role of mRNA stability proteins in regulation of vascular response to injury, as well as their modification by anti-inflammatory factors represent the second gap in our knowledge on how anti-inflammatory interleukins may be atheroprotective.

IL-19 has inflammation-dampening effects on cultured VSMC and endothelial cell, including reduction of expression of proinflammatory cytokines and adhesion molecules.[5,9,12] Collectively, these studies suggest that IL-19 expression in atherosclerotic plaque may be a compensatory, counter-regulatory mechanism to reduce local inflammation. However, an investigation into the absence of IL-19 on the development of atherosclerosis has not been tested or reported.

We hypothesized that genetic deletion of IL-19 would augment atherosclerosis in *Ldlr*$^{-/-}$ mice. To test this hypothesis, we crossed *Il19*$^{-/-}$ mice with *Ldlr*$^{-/-}$ to create double knockout (dKO) mice. In this study, we report that loss of IL-19 leads to exacerbated atherosclerosis, which can be rescued by treatment with recombinant mouse IL-19 in dKO mice. Further, we report that a potential mechanism for these effects is an increase in proinflammatory gene mRNA stability in bone marrow-derived macrophage (BMDM) and VSMC in dKO mice. IL-19 regulation of mRNA stability may be mediated by miRNA targeting of mRNA stability proteins. From a broader perspective, this study also suggests that mRNA stability proteins may represent targets for novel antiatherosclerotic therapeutics.

Materials and Methods

A detailed listing of mice and antibodies used are listed in the major resource table in the online-only Data Supplement.

Mouse Studies

Ldlr$^{-/-}$ mice on the C57BL/6 background purchased from Jackson laboratories (Catalog number 002207) were bred with *Il19*$^{-/-}$ mice previously described[10,11] to obtain homozygous *Il19*$^{-/-}$×*Ldlr*$^{-/-}$ dKO mice. Mice were housed in an ALAC-approved facility and maintained on a standard chow diet until study commencement. Mice of both sexes were entered in the study at 8 weeks of age when normal chow was replaced with an atherogenic diet (42% fat, 0.2% cholesterol, Harlan atherogenic diet TD.88137). For the rescue study, mice were injected IP with 10 ng/g per day recombinant mouse IL-19 (BioVision, Catalog number 4546) as we have described[10,11] or an equal volume of PBS, 5 days per week for 14 weeks. Fasting lipid content in mouse sera was analyzed by Charles River Research Animal Diagnostic Services. For adaptive bone marrow transplantation, 8-week-old male and female *Ldlr*$^{-/-}$ mice were irradiated (950 rads). Bone marrow was isolated from *Ldlr*$^{-/-}$ and dKO donors as described below and transplanted via single retro-orbital injection (5 million cells/injection). After 4 weeks, mice were administered atherogenic diet for 14 weeks. All animal procedures adhered to approved Temple University Institutional Animal Care and Use Committee approved protocols.

Atherosclerotic Lesion Analysis

Atherosclerotic plaque burden was determined in the aortic intimal surface by en face staining with Sudan IV and in the aortic root by Oil Red O staining as we described.[10,11] Lesion size in the aortic arch was determined by quantitative morphometry using the Image Pro Plus program. Aortic root was frozen in optimal cutting temperature medium and sectioned. Four transverse serial sections spaced 70 to 100 µm apart from the aortic sinus to disappearance of valve cusps per aortic root were stained with Oil Red O, and positive stained areas quantitated as a percentage of total area by quantitative morphometry.

Cell Culture

Aorta from *Ldlr*$^{-/-}$ and dKO mice were excised, endothelial layer removed, and VSMC isolated as we described.[6,12,13] VSMC were cultured in DMEM supplemented with 20% fetal bovine serum (FBS). Over 95% of isolated cells were SMC actin positive, and VSMC from passage 2 to 4 were used. For BMDM, femurs and tibiae were flushed with sterile PBS, red blood cells were lysed and removed using ACK lysis buffer (ThermoFisher) and cell strainers. Collected cells were resuspended and seeded in DMEM+10% heat-inactivated FBS with 100 ng/mL M-CSF (Peprotech). Cells were cultured for 6 to 7 days until confluent. For gene and protein expression analyses, cells were stimulated with 10 ng/mL TNF (tumor necrosis factor)-α (Sigma). For RNA stability experiments, cells were treated with 10 ng/mL actinomycin D after TNF-α stimulation. Untreated samples were used as controls.

RNA Extraction and Quantitative RT-PCR

RNA from spleen, aortic arch, and cultured cells was isolated using the RNeasy PowerLyzer Tissue & Cells Kit (Qiagen) and Direct-zol RNA Miniprep Plus (Zymo Research) for tissue and cells, respectively, according to the manufacturer's protocol. A full description of RT-PCR is found in the online-only Data Supplement.

Western Blotting

Protein extracts made as described were separated by SDS-PAGE, transferred to nitrocellulose membrane, incubated with a 1:3000 dilution of primary antibody HuR or TNF-α (Abcam, Santa Cruz Biotechnology), followed by a 1:4000 dilution of secondary antibody.[4,6,9,10,12] A full description of Western blotting is found in the online-only Data Supplement.

Immunohistochemistry

Aortic roots were frozen in optimal cutting temperature and 5 µm-thick serial sections were cut and placed on microscope slides.[4,9,10,12,13] A full description of the immunohistochemical methodology is found in the online-only Data Supplement.

Intracellular Staining and Flow Cytometry

Flow cytometry analysis was performed on whole blood from mice to detect TNF-α in peripheral blood lymphocytes. A full description of intracellular staining and Flow cytometry is found in the online-only Data Supplement.

Statistical Analysis

Results are expressed as mean±SEM. A full description of statistical analysis is found in the online-only Data Supplement.

Results

Il19$^{-/-}$×*Ldlr*$^{-/-}$ dKO Mice Have Increased Atherosclerotic Plaque

Il19$^{-/-}$ mice were crossed with *Ldlr*$^{-/-}$ mice. DKO and age and sex-matched *Ldlr*$^{-/-}$ mice were fed high-fat diet (HFD) for 14 weeks, and atherosclerotic surface lesion area was determined by en face staining of the aortic arch and quantitative morphometry. DKO mice had significantly greater plaque surface area compared with *Ldlr*$^{-/-}$ control mice (13.41±1.0% in *Ldlr*$^{-/-}$ versus 21.1 3±1.2% in dKO; $P<0.0001$; Figure 1A and 1B). Lesion area was also assessed in transverse sections of Oil Red O-stained aortic root, which demonstrates significantly increased lesion area in dKO mice compared with *Ldlr*$^{-/-}$ controls (16.34±2.5% in *Ldlr*$^{-/-}$ versus 26.11±3.7% in dKO; $P<0.05$; Figure 1C and 1D). There was no significant difference in lesion area between sexes in either group. There was also no significant difference in lipid profile (cholesterol: 2155±325.9 mg/dL in *Ldlr*$^{-/-}$ versus 2044±487 mg/dL in dKO; triglyceride: 925.4±243 mg/dL in *Ldlr*$^{-/-}$ versus 1022±392.2 mg/dL in dKO; Figure 1E) or weight gain during the course of the study (6.033±1.5 g in *Ldlr*$^{-/-}$ versus 5.346±1.2 g in dKO; Figure 1F; Figure I in the online-only Data Supplement). Together these data suggest that absence of IL-19 results in increased severity of atherosclerosis.

Recombinant IL-19 Treatment Rescues dKO Atherosclerotic Phenotype

To confirm the role of IL-19 in atherogenesis and to demonstrate the specificity of IL-19, dKO mice were administered daily IP injections of recombinant mouse IL-19 (10 ng/g per day), or an equivalent volume of phosphate buffered saline while simultaneously being fed HFD for 14 weeks. En face staining of aorta shows that dKO mice injected with IL-19 had significantly less plaque burden compared with dKO mice injected with saline (23.89±3.8% in PBS injected versus 11.72±1.1% in IL-19 injected; $P<0.01$; Figure 1G and 1H). As in the previous experiment, there were no significant differences in serum lipid profile or weight gain between IL-19 and saline-injected mice. Because the addition of IL-19 to dKO mice can rescue, or decrease atherosclerosis burden, these data demonstrate IL-19 specificity and suggest that IL-19 can regulate development of atherosclerosis.

Loss of IL-19 Influences Global and Local Inflammatory Responses

The development and severity of atherosclerosis is influenced by systemic adaptive immunity as well as local adaptive immunity within the plaque. To determine whether loss of IL-19 had systemic and local effects on the adaptive immune response, spleen and aorta were harvested from *Ldlr*$^{-/-}$ and dKO mice after 14 weeks of HFD feeding, at the time of euthanasia. Markers associated with T cell and macrophage polarity were quantitated by qRT-PCR. Figure 2A shows significantly increased levels of mRNA of several proinflammatory markers in dKO spleen, including TNF-α, TBet, IL-12β, and IL-1β, suggesting a globally polarized T_h1, M1 profile in dKO mice. Correspondingly, there was significantly decreased expression of Tregs marker, FOXP3, and anti-inflammatory cytokine, IL-10 in spleen from dKO mice. There were no significant differences in GATA3, Arg2, or Arg1 mRNA in spleen between dKO and control mice, suggesting no differences in T_h2 or M2 populations in spleen (Figure II in the online-only Data Supplement). Similarly, Figure 2C displays significantly increased TNF-α, TBet, Arg2, IL-12β, IL-1β, MCP-1, and RORγ mRNA abundance in the aortic arch from dKO compared with *Ldlr*$^{-/-}$ mice, indicating an immune profile within the plaque polarized to T_h1, T_h17, and M1. Interestingly, an abundance of T_h2 marker, GATA3, and IL-10 mRNA were significantly decreased in the aortic arch of dKO mice. Despite differences in macrophage polarization, no significant difference was noted in a total number of infiltrating macrophages in the atherosclerotic lesions of dKO mice compared with control mice (Figure IV in the online-only Data Supplement).

Treatment of dKO mice with IL-19 was able to rescue the immune cell profile in the spleen, as Figure 2B shows significantly decreased levels of TNF-α, TBet, IL-12β, and IL-1β mRNA, as well as significantly increased FOXP3 and IL-10 mRNA when compared with dKO mice treated with saline. Figure 2D shows that aortic arch from dKO mice treated with IL-19 has significantly decreased TNF-α, TBet, Arg2, IL-12β, MCP-1, RORγ, and IL-1β mRNA, and significantly greater levels of GATA3 and IL-10 mRNA compared with PBS injected control mice. When taken together, this data suggests that mice receiving IL-19 treatment have decreased T_h1, T_h17, and M1 associated gene expression both systemically and locally, compared with saline-treated controls, and suggests that differences in plaque severity in dKO mice compared with *Ldlr*$^{-/-}$ controls may be mediated by both systemic and intraplaque polarization of adaptive immunity. Raw numbers for all qRT-PCR are shown in Tables I and II in the online-only Data Supplement.

The effects of deletion of IL-19 on circulating immune cells was determined by flow cytometry. There is no difference in the number of circulating IFNγ+ or FoxP3+ T cells, nor TNF-α+ or CD206+ macrophages in *Ldlr*$^{-/-}$ and dKO mice after 14 weeks of HFD (Figure IIIA in the online-only Data Supplement). However, we did observe a significantly greater percentage of TNFα+ CD4 T cells in dKO mice compared with *Ldlr*$^{-/-}$ controls, consistent with T_h1, M1 polarization observed in spleen and aortic arch from dKO mice. We observed no differences in total numbers of circulating leukocytes, including lymphocytes, neutrophils, and monocytes in these mice (Figure IVB in the online-only Data Supplement).

Immune Cells Participate in IL-19 Antiatherosclerotic Effects

IL-19 has confirmed immunoregulatory effects, and it was important to determine the major effector cell of IL-19

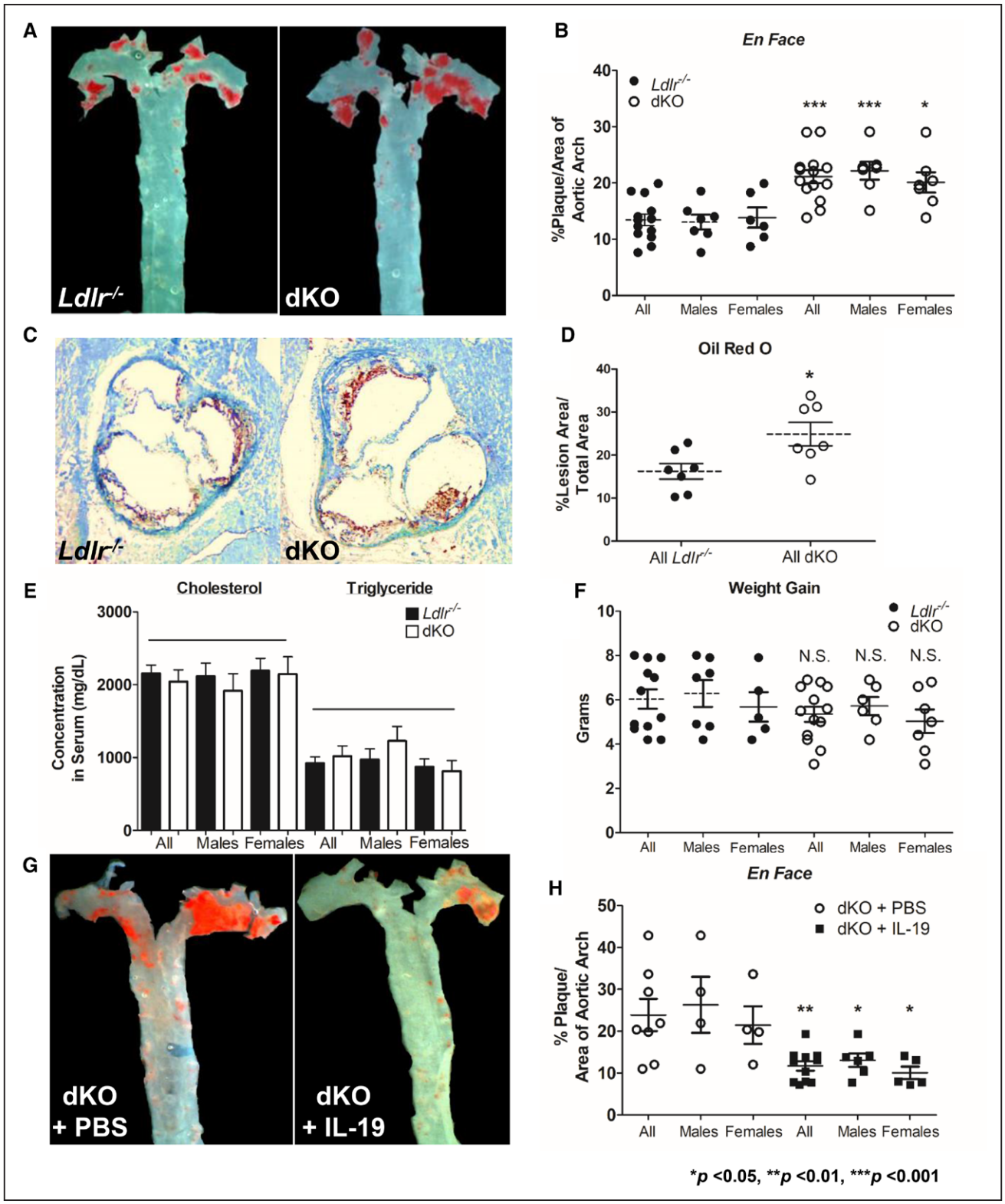

Figure 1. Genetic deletion of IL (interleukin)-19 exacerbates atherosclerosis. **A**, Representative photomicrograph of aortic arch from *Ldlr*$^{-/-}$ and double knockout (dKO) mice after consuming high-fat diet (HFD) for 14 wk. Surface lesions en face stained with Sudan IV. **B**, Graphic depiction of atherosclerotic lesion size quantitated from en face stained aortic arches as depicted in **A** (n=13 *Ldlr*$^{-/-}$ vs 14 dKO). **C**, Representative photomicrographs of aortic root stained with Oil Red O from *Ldlr*$^{-/-}$ and dKO mice after 14 wk of HFD. **D**, Quantitation of percent positive Oil Red O-stained lesion areas from 4 transverse serial sections of aortic root (n=7 per group). **E**, Cholesterol and triglyceride levels in circulating plasma do not statistically differ between *Ldlr*$^{-/-}$ and dKO mice after 14 wk of HFD (n=8 per group). **F**, *Ldlr*$^{-/-}$ and dKO mice do not statistically differ in weight gained after 14 wk of HFD feeding. Injection of IL-19 rescues dKO phenotype and reduces atherosclerosis. **G**, Representative photomicrograph of aortic arch surface from dKO mice injected with either 10 ng/g per d IL-19 or PBS while being fed HFD for 14 wk; surface lesions en face stained with Sudan IV. **H**, Graphic depiction of atherosclerotic lesion size quantitated from en face stained aortic arches as depicted in **G** (n=8 dKO+PBS vs 11 dKO+IL-19).

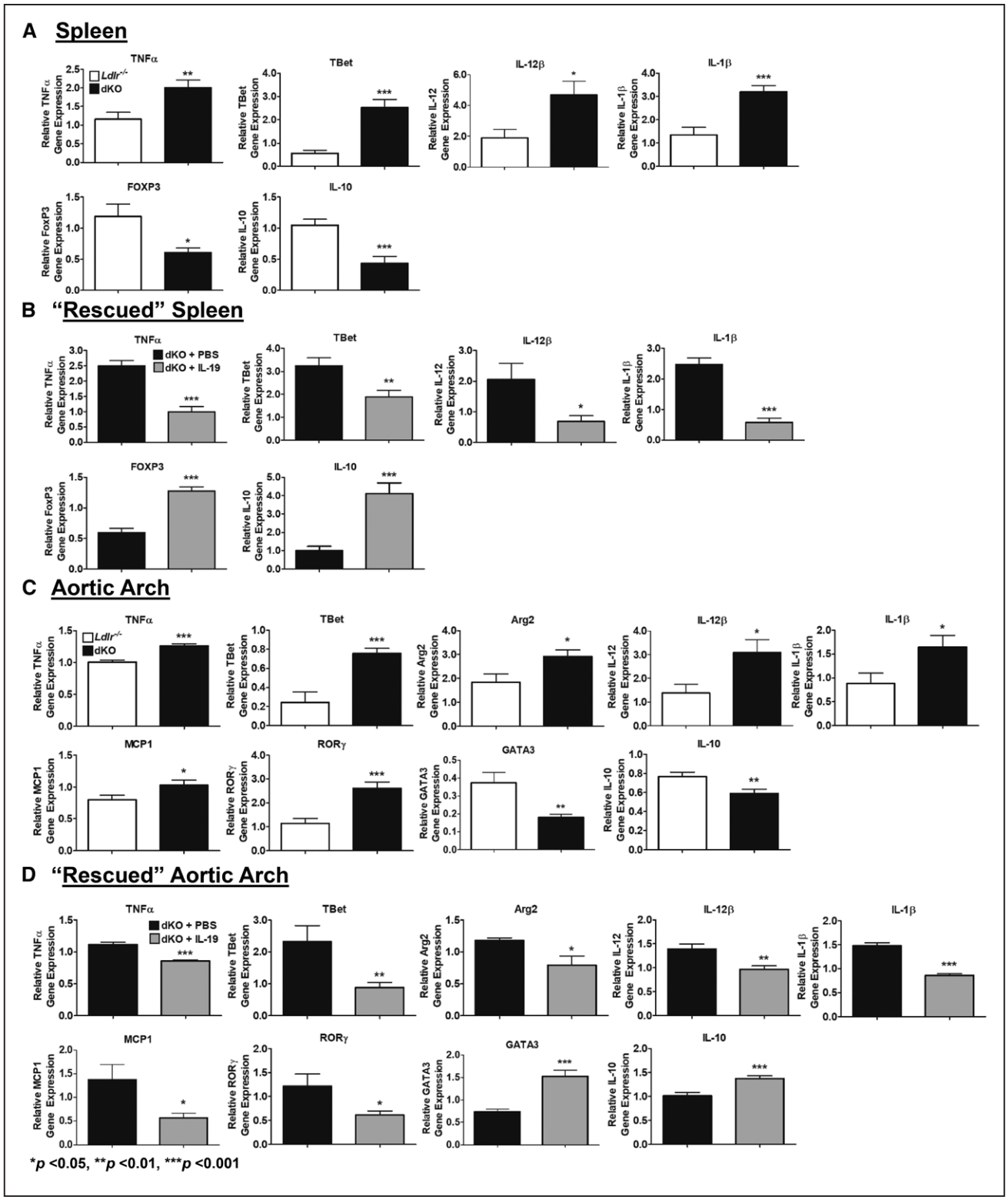

Figure 2. Deletion of IL (interleukin)-19 polarizes the systemic and local immune responses. IL-19 treatment is able to rescue phenotype. Quantitative RT-PCR analysis of spleen and aortic arch harvested from *Ldlr*$^{-/-}$ and dKO mice after 14 wk of high-fat diet (HFD; **A**, **C**) and double knockout (dKO) mice simultaneously injected with IL-19 or PBS during HFD feeding (**B**, **D**). At the time of euthanasia, RNA was extracted, reverse transcribed, and amplified using primers for the genes shown. (n=8 spleen, aortic arch per group).

atheroprotection. To this end, dKO mice were transplanted with bone marrow isolated from dKO or *Ldlr*$^{-/-}$ control mice and fed HFD for 14 weeks. En face analysis indicates that mice receiving dKO BM had significantly more atherosclerotic lesion area compared with control mice (8.46±0.63% for *Ldlr*$^{-/-}$ versus 12.62±0.85% for dKO; $P<0.01$; Figure 3A

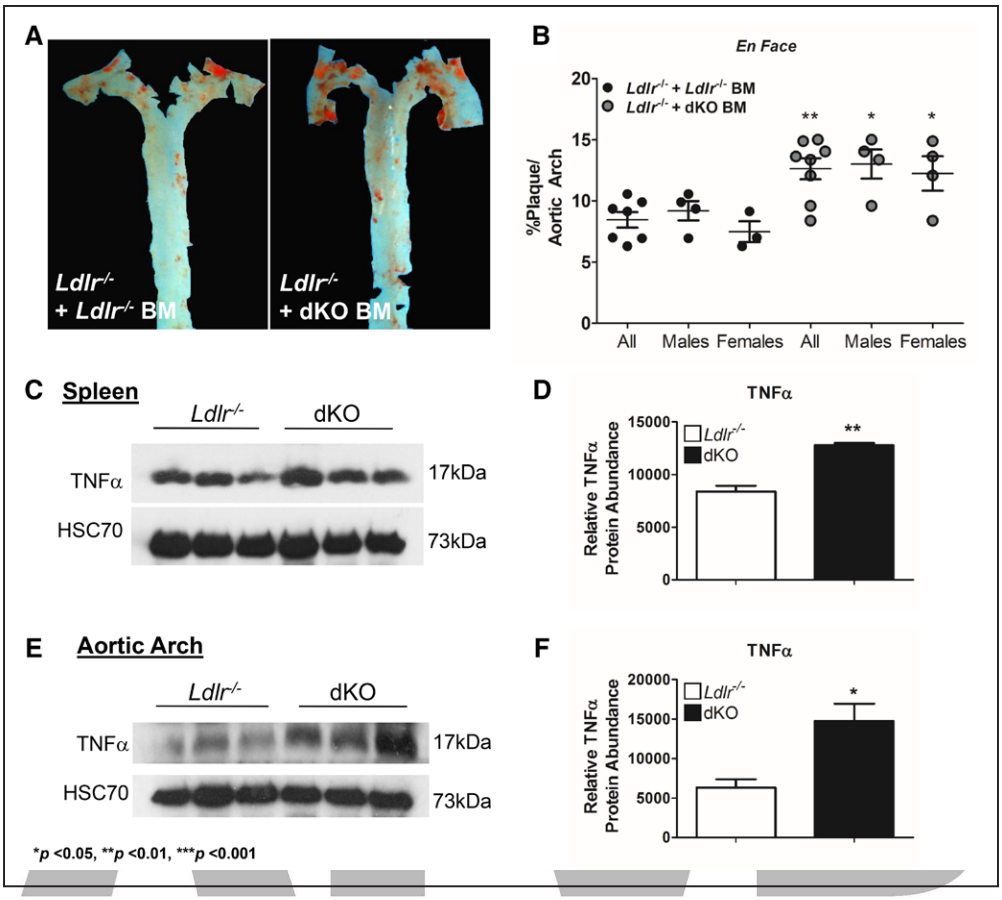

Figure 3. Immune cells participate in IL (interleukin)-19 mediated atheroprotection. **A**, Representative photomicrograph of aortic arch from *Ldlr*$^{-/-}$ transplanted with *Ldlr*$^{-/-}$ or double knockout (dKO) bone marrow (BM), after consuming high-fat diet (HFD) for 14 wk. Surface lesions en face stained with Sudan IV. **B**, Graphic depiction of atherosclerotic lesion size quantitated from en face stained aortic arches as depicted in **A** (n=7 *Ldlr*$^{-/-}$ recipients vs 8 dKO recipients). Deletion of IL-19 increases TNF (tumor necrosis factor)-α expression. Increased TNF-α protein expression in the spleen (**C**) and aortic arch (**E**) of dKO mice compared with *Ldlr*$^{-/-}$ mice after 14 wk of HFD, determined by immunoblot and consequent densitometry (**D**, **F**). (n=3 spleen, aortic arch per group).

and 3B). This suggests that immune cells participate in IL-19 mediated atheroprotection.

Loss of IL-19 Increases TNF-α Expression and Stability in BMDM and VSMC

TNF-α is a potent proinflammatory cytokine that participates in atherogenesis.[14] TNF-α protein abundance was significantly elevated in the spleen of dKO mice after 14 weeks of HFD compared with *Ldlr*$^{-/-}$ control mice (838±56 AU in *Ldlr*$^{-/-}$ versus 1276±20 AU in dKO; $P<0.001$; Figure 3C and 3D). Similarly, TNF-α protein was increased in the aortic arch of dKO mice compared with *Ldlr*$^{-/-}$ control mice (630.7±107 AU in *Ldlr*$^{-/-}$ versus 1471±221 AU in dKO; $P<0.05$; Figure 3E and 3F). These data suggest dKO mice have both a global and local increase in proinflammatory TNF-α expression.

To determine the molecular mechanisms that may be responsible for the increased abundance of TNF-α in dKO mice, we isolated BMDM and VSMC from *Ldlr*$^{-/-}$ and dKO mice. BMDM and VSMC were cultured and stimulated with TNF-α, a potent proinflammatory stimulus. Both BMDM and VSMC from dKO mice expressed significantly increased amounts of TNF-α mRNA compared with *Ldlr*$^{-/-}$ controls (BMDM: 88.10±4.62 AU in *Ldlr*$^{-/-}$ versus 190.5±3.093 AU in dKO, $P<0.001$; VSMC: 5.098±0.775 AU in *Ldlr*$^{-/-}$ versus 10.54±0.309 AU in dKO, $P<0.01$; Figure 4A and 4G). To further define a mechanism, this experiment was repeated with the addition of the transcription inhibitor actinomycin D after TNF-α stimulation. TNF-α mRNA was significantly more stable in cells isolated from dKO mice compared with *Ldlr*$^{-/-}$ control mice (Figure 4B and 4H). To confirm the specificity of IL-19 in regulating TNF-α mRNA stability, we next attempted to rescue increased TNF-α mRNA stability in dKO cells by pretreating them with IL-19. Pretreatment with IL-19, before TNF-α stimulation in dKO BMDM and VSMC significantly decreases TNF-α mRNA stability when compared with control dKO cells (Figure 4C and 4I). We examined mRNA transcripts of additional proinflammatory cytokines known to participate in atherogenesis and also regulated by IL-19. Similar results were obtained with IL-1β in BMDM, and MCP-1 in VSMC (Figure 4E, 4F, 4K, and 4L, respectively). These data suggest that IL-19 can control proinflammatory cytokine abundance in BMDM and VSMC by regulation of mRNA stability.

HuR Is Elevated in Mice Lacking IL-19

Regulation of mRNA stability is an important post-transcriptional mechanism of controlling inflammatory cytokine

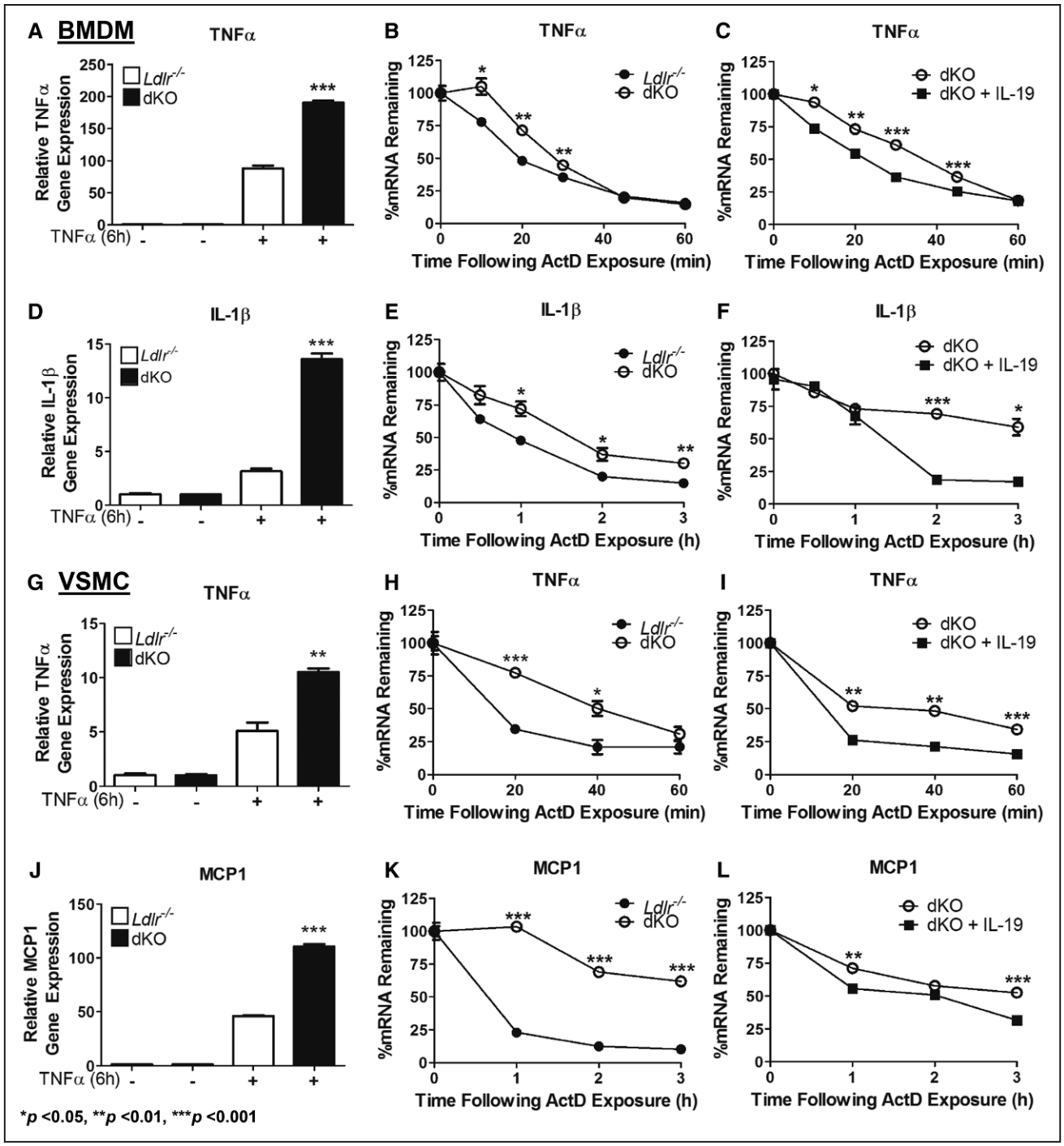

Figure 4. Deletion of IL (interleukin)-19 increases expression and mRNA stability of proinflammatory transcripts. Bone marrow-derived macrophages (BMDM) and vascular smooth muscle cell (VSMC) were cultured from *Ldlr*$^{-/-}$ and double knockout (dKO) mice. Cells were stimulated with TNF (tumor necrosis factor)-α to induce expression of proinflammatory cytokines. **A**, **D**, **G**, **J**, Quantitative RT-PCR was performed on BMDM and VSMC. DKO BMDM and VSMC both demonstrate increased expression of TNF-α, as well as IL-1b and MCP-1 in each respective cell type, compared with *Ldlr*$^{-/-}$ controls (n=3 per group). **B**, **E**, **H**, **K**, The transcription inhibitor actinomycin D was added at varying times after addition of TNF-α. Quantitative RT-PCR was utilized and values were normalized to time point 0 to determine percentages of mRNA remaining over time. DKO BMDM express more stable TNF-α and IL-1b mRNA and dKO VSMC express more stable TNF-α and MCP-1 over time than *Ldlr*$^{-/-}$ controls (n=3 per group). **C**, **F**, **I**, **L**, Pretreatment with IL-19 before TNF-α stimulation to dKO BMDM and VSMC results in significant reduction of TNF-α, IL-1b, and MCP-1 RNA stability. (n=3 per group).

abundance. HuR (human antigen R) is an important regulator of TNF-α mRNA stability,[15,16] and because IL-19 treatment resulted in decreased proinflammatory cytokine mRNA stability, several experiments were performed to draw a relationship between IL-19 expression and HuR abundance. First, we determined if HuR is expressed in murine atherosclerotic plaque. Immunohistochemical localization shows that HuR is expressed more robustly in the area of the plaque,

rather than in the media, distal from the plaque. Dual-color immunohistochemistry using lineage-specific antibody shows that HuR expression is similar to IL-19 in that it is expressed in VSMC, macrophages and EC[10] (Figure V in the online-only Data Supplement). Next, HuR mRNA and protein abundance in spleen and aortic arch from *Ldlr*$^{-/-}$ and dKO mice fed 14 weeks of HFD were quantitated. Figure 5A demonstrates that HuR mRNA is significantly increased in spleen from dKO mice compared with *Ldlr*$^{-/-}$ controls (1.15±0.2 AU in *Ldlr*$^{-/-}$ versus 2.83±0.4 AU in dKO; $P<0.01$). Figure 5B and 5C show that HuR protein is also significantly greater in dKO spleen (623±22.7 AU in *Ldlr*$^{-/-}$ versus 1081±69.9 AU in dKO; $P<0.001$). Figure 5D through 5F display that both HuR mRNA and protein are significantly increased in the aortic arch of the dKO compared with *Ldlr*$^{-/-}$ mice (mRNA: 0.77±0.02 AU in *Ldlr*$^{-/-}$ versus 1.17±0.2 AU, $P<0.001$; protein: 326.0±26 AU in *Ldlr*$^{-/-}$ versus 864.7±23 AU, $P<0.001$). Cultured BMDM

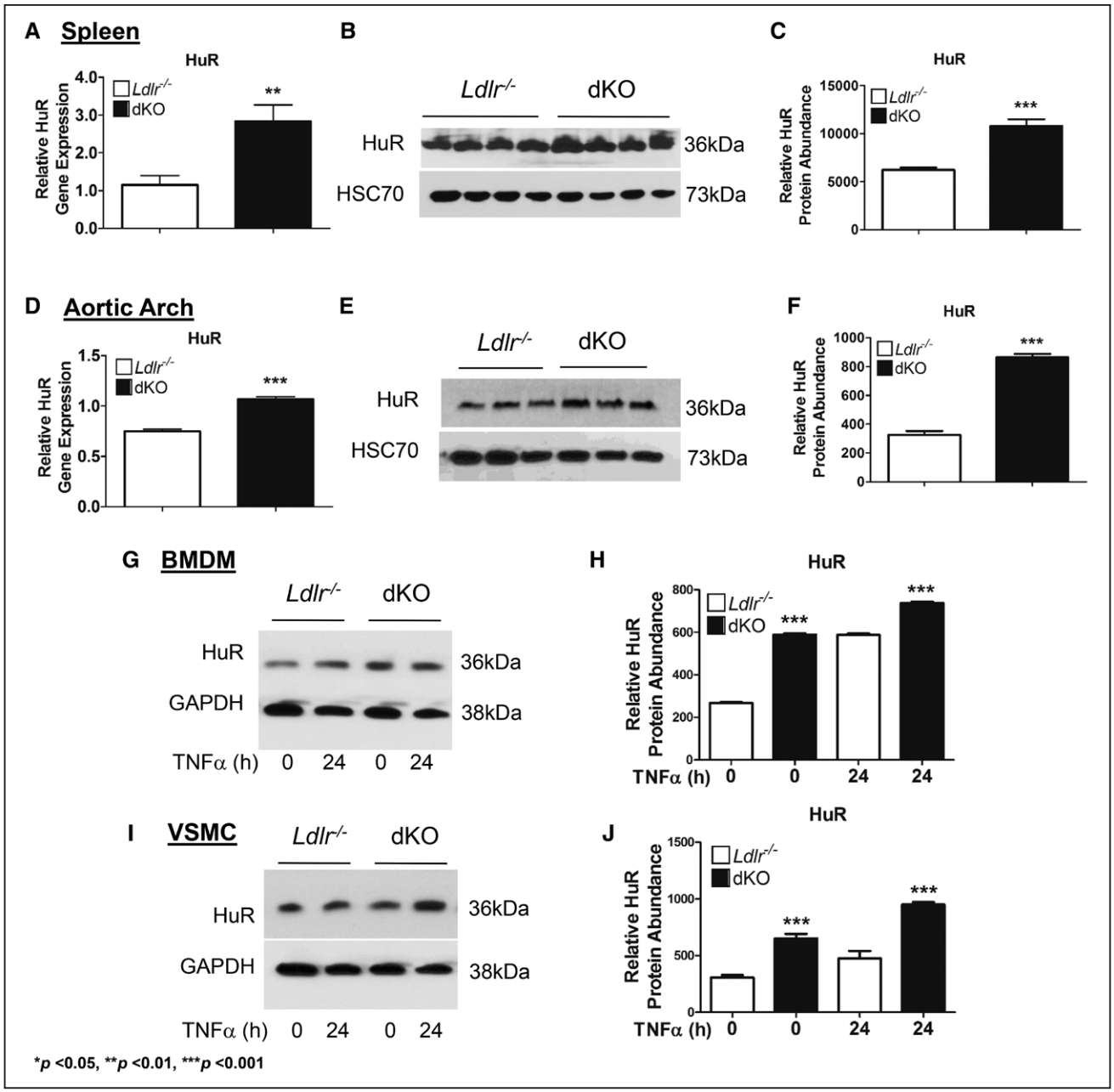

Figure 5. Deletion of IL (interleukin)-19 results in increased HuR (human antigen R) abundance. Spleen and aortic arch were harvested from *Ldlr*$^{-/-}$ and double knockout (dKO) mice after 14 wk of high-fat diet (HFD), at the time of euthanasia. **A**, **D**, HuR mRNA expression is significantly increased in the spleen and aortic arch of dKO mice compared with *Ldlr*$^{-/-}$ controls (n=8 spleen, aortic arch per group). **B**, **E**, DKO spleen and aortic arch express significantly greater HuR protein levels compared with *Ldlr*$^{-/-}$ controls determined by immunoblot. **C**, **F**, Relative HuR protein abundance in **B** and **E** quantitated by densitometry. (n=4 spleen, n=3 aortic arch per group). **G–J**, Protein lysates from bone marrow-derived macrophage (BMDM) and VSMC stimulated with TNF (tumor necrosis factor)-α for 24 h and unstimulated controls were immunoblotted with anti-HuR antibody (**G**, **I**) and expression quantitated by densitometry (**H**, **J**). DKO BMDM and VSMC express significantly greater levels of HuR protein than *Ldlr*$^{-/-}$ mice (n=4 per group).

from dKO mice stimulated with TNF-α express significantly increased HuR protein levels compared with BMDM from *Ldlr*$^{-/-}$ mice (Figure 5G and 5H). Interestingly, unstimulated BMDM from dKO express significantly higher basal levels of TNF-α compared with BMDM from *Ldlr*$^{-/-}$. Similarly, VSMC explanted from dKO also express significantly greater levels of HuR under basal conditions, as well as after TNF-α stimulation when compared with *Ldlr*$^{-/-}$ VSMC (Figure 5I and 5J). These data suggest that absence of IL-19 is associated with an increase in HuR mRNA and protein abundance.

IL-19 Treatment Reduces HuR mRNA Stability

We utilized BMDM and VSMC explanted from *Ldlr*$^{-/-}$ and dKO mice to determine a mechanism for the observed effect of IL-19 on HuR abundance. Using actinomycin D, we observed significantly increased stability of HuR mRNA in both BMDM and VSMC from dKO mice compared with *Ldlr*$^{-/-}$ controls (Figure 6A and 6D). We next added recombinant mouse IL-19 to dKO cells to rescue HuR mRNA stability. Figure 6B and 6E show that treatment with IL-19 to dKO BMDM and VSMC significantly decreases HuR mRNA stability in the dKO cells, compared with control cells that were not treated with IL-19.

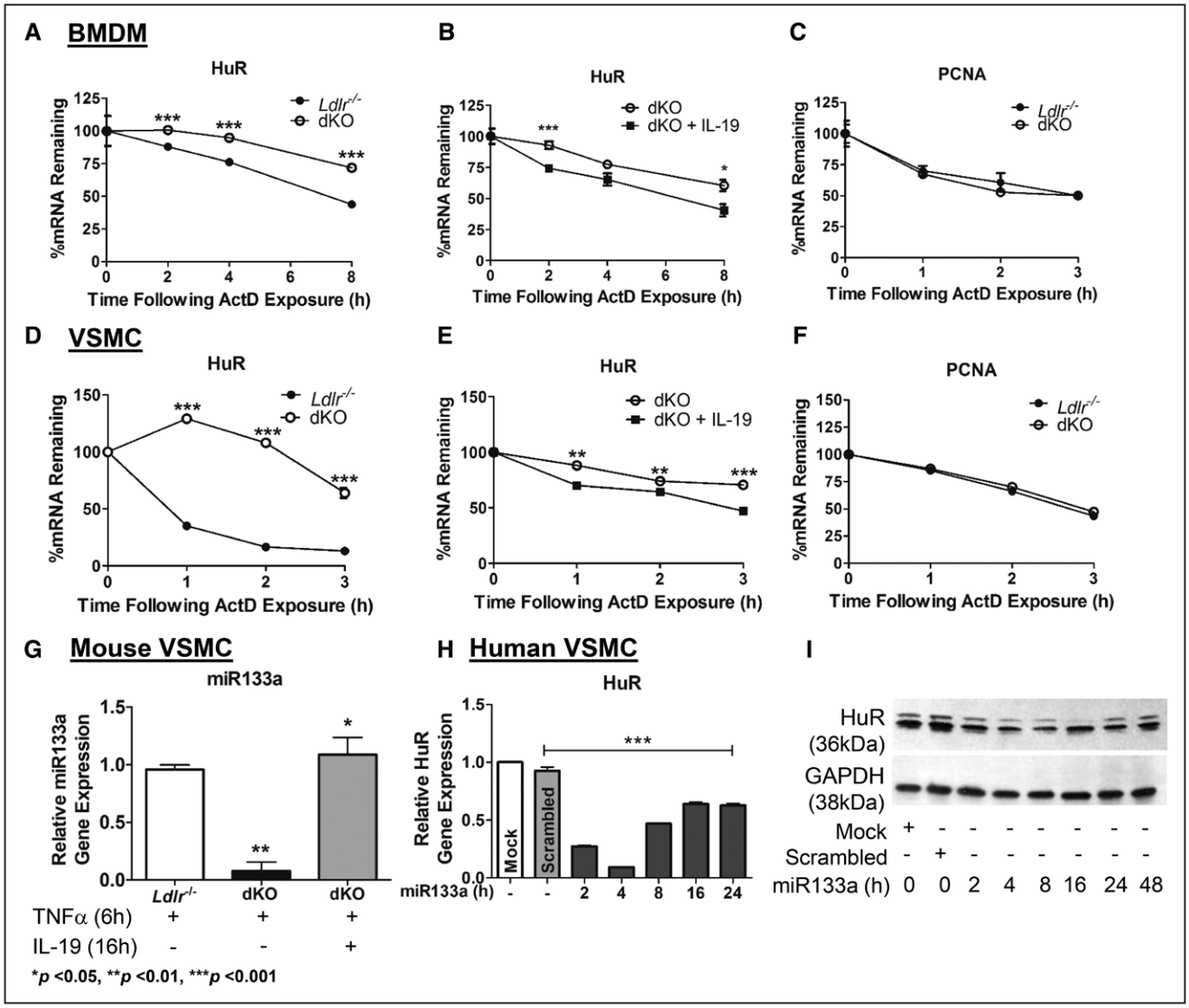

Figure 6. Deletion of IL (interleukin)-19 increases mRNA stability of HuR (human antigen R). Bone marrow-derived macrophage (BMDM) and vascular smooth muscle cell (VSMC) were cultured from *Ldlr*$^{-/-}$ and double knockout (dKO) mice. Cells were stimulated with TNF (tumor necrosis factor)-α and the transcription inhibitor actinomycin D was added at varying times after stimulation. Quantitative RT-PCR was performed and values were normalized to time point 0 to determine percentages of HuR mRNA remaining over time. **A**, **D**, Loss of IL-19 results in significantly increased stability of HuR mRNA in dKO BMDM and VSMC. (n=3 per group). **B**, **E**, Pretreatment with IL-19 before TNF-α stimulation of dKO BMDM and VSMC results in significantly decreased the stability of HuR mRNA (n=3 per group). **C**, **F**, qRT-PCR analysis showing the stability of proliferating cell nuclear antigen (PCNA) mRNA, which lacks AU-rich elements (AREs) in the 3′UTR, in *Ldlr*$^{-/-}$ and dKO BMDM and VSMC stimulated with TNF-α (n=3 per group). **G**, dKO VSMC stimulated with TNF-α express lower levels of muscle-specific miRNA, miR133a, compared with *Ldlr*$^{-/-}$ control VSMC. Pretreatment with IL-19 is able to rescue levels of miR133a in dKO VSMC (n=3 per group). **H**, Time course showing HuR mRNA is significantly decreased after transfection with miR133a mimic in human VSMC. RNA was extracted at the indicated times after transfection, and HuR mRNA abundance detected by qRT-PCR. **I**, Time course showing HuR protein is significantly decreased following transfection with miR133a mimic in human VSMC. Cell lysates were Western blotted using the indicated antibodies.

Proliferating cell nuclear antigen, which lacks AU-rich elements (AREs) in its 3′ untranslated region (UTR) served as a negative control and Figure 6E and 6F demonstrate no difference in proliferating cell nuclear antigen mRNA stability between *Ldlr*$^{-/-}$ and dKO BMDM and VSMC. Together, these data strongly suggest that IL-19 can decrease HuR mRNA stability, and the increase in HuR noted in dKO mice and cells isolated from dKO mice is likely because of loss of IL-19.

It was important to determine a more detailed mechanism of how IL-19 might decrease HuR mRNA stability. We previously described that IL-19–induced expression of miR133a, a muscle-specific miRNA, in human VSMC.[17] In searching a public database (http://www.targetscan.org) one predicted target for miR133a is HuR 3′UTR (Data VIA in the online-only Data Supplement). To determine whether this was a mechanism for differences in HuR abundance, we found that dKO VSMC expressed significantly less miR133a compared with *Ldlr*$^{-/-}$ control VSMC. miR133a expression trended lower in dKO compared with control aorta (Data VIB in the online-only Data Supplement). Importantly, miR133a expression could be induced or rescued in dKO VSMC by the addition of IL-19 (Figure 6G). Figure 6H shows that transfection of miR133a significantly reduced HuR mRNA abundance in hVSMC, and Figure 6H validates this at the protein level, suggesting that one potential mechanism for the IL-19 reduction in HuR abundance is mediated by miR133a expression.

Discussion

The major finding from this study is that the absence of the anti-inflammatory cytokine IL-19 results in increased atherosclerosis, which can be reversed by injection of recombinant mouse IL-19 into the *Il19*$^{-/-}$ x *Ldlr*$^{-/-}$ dKO mice. T_h1 interleukins are considered to be proinflammatory and proatherogenic, and in general, T_h2 interleukins are proposed to be antiatherogenic.[14,18–20] Thus, alteration in the balance of these interleukins could potentially affect the development and severity of atherosclerosis. Previous studies led us to hypothesize that IL-19 may represent a counter-regulatory mechanism to reduce local inflammation. The present study showed increased systemic and intraplaque expression of the proinflammatory cytokine TNF-α in *Ldlr*$^{-/-}$ mice lacking IL-19. Importantly, injection of IL-19 into dKO mice significantly reduced plaque burden to levels comparable to *Ldlr*$^{-/-}$ mice, confirming atheroprotective effects and validating the specificity of IL-19 in this system.

Genetic deletion of the archetypal T_h2 interleukin IL-10 also reduces atherosclerosis formation in several studies,[21,22] but there are some notable differences from loss of IL-19. In *Il10*$^{-/-}$ mice crossed into the ApoE background, total cholesterol was higher in the dKO mice, where in our study no difference in cholesterol between *Ldlr*$^{-/-}$ and dKO was noted.[22,23] The anti-inflammatory cytokine, IL-33 also induces T_h2 cytokine responses, and injection of IL-33 into ApoE mice has been shown to ameliorate the development of atherosclerosis.[25] In both of these cases, authors concluded that protection was because of adaptive immune modulation.

TNF-α is considered to be a master inflammatory cytokine as it induces expression of multiple proinflammatory genes.[24] A significantly greater amount of circulating TNF-α+ CD4+ T cells in dKO compared with *Ldlr*$^{-/-}$ mice following 14 weeks of HFD consumption suggested systemic effects of IL-19. This was confirmed as spleen from dKO mice had increased expression of TNF-α mRNA and protein, and TBet expression was increased in the dKO spleen compared with *Ldlr*$^{-/-}$. Differences in intraplaque gene expression were more pronounced than systemic differences; in addition to an increased TBet expression which was seen in spleen, GATA3 was reduced and Arg2 was increased within the aortic arch, indicating a local reduction in T_h2 T cells and an increase in proinflammatory M1 macrophages. Importantly, aortic arch from dKO mice had a significantly greater expression of TNF-α protein compared with controls. The antiatherosclerotic effects of IL-19 are unique in that they seem to be both indirect and direct by affecting adaptive immune responses and by dampening inflammation in macrophages and VSMCs within the plaque area. It was interesting to note that there was less IL-10 mRNA expression in dKO aortic arch compared with controls. This may be a direct effect of loss of IL-19 and an additional cause for exacerbated plaque size; decreased levels of IL-10 can be considered to be a contributing factor, as IL-10 has antiatherosclerotic effects.[22,23] Concordant with that observed for *Ldlr*$^{-/-}$ and dKO mice, the immune cell profile in the aortic arch of dKO mice rescued with IL-19 resembled that of *Ldlr*$^{-/-}$ mice, demonstrating localized anti-inflammatory effects of IL-19.

With this in mind, it was important to determine whether IL-19 antiatherosclerotic effects were mediated by the polarization of adaptive immunity or by direct anti-inflammatory effects on resident vascular cells. Transplantation of dKO BM into *Ldlr*$^{-/-}$ mice results in significantly increased plaque size compared with control BM. This confirms that at least some of IL-19 atheroprotective effects are mediated by immune cells. This is not surprising as IL-19 is a Th2 interleukin with confirmed immunomodulatory activity.[25–28] When taken together, IL-19 antiatherosclerotic effects are likely both indirect, by effecting adaptive immune responses, and direct, by dampening inflammation in macrophages and VSMCs within the plaque area.

An additional feature distinguishing IL-19 from IL-10 and IL-33 is that IL-19 is expressed in VSMC as well as immune cells; how the absence of IL-19 affects the response of these cells to inflammatory stimuli has not been reported. We explanted BMDM and VSMC from dKO and *Ldlr*$^{-/-}$ mice to closely characterize the inflammatory response in each. In both cell types, the cells lacking IL-19 had an increased inflammatory response to TNF-α stimulation. More detailed analysis determined that loss of IL-19 resulted in increased proinflammatory cytokine mRNA stability, which could be reversed, or rescued by addition of IL-19 to dKO BMDM and VSMC. Although this does not rule out transcriptional effects, it does reveal that one mechanism for IL-19 anti-inflammatory activity takes place post-transcriptionally. Reduction of proinflammatory cytokine mRNA stability by IL-19 is consistent with our hypothesis that IL-19 acts as a compensatory, negative regulatory factor in response to inflammatory stimuli.

TNF-α is an example of a potent, rapid-response proinflammatory cytokine whose mRNA stability is post-transcriptionally regulated by RBPs (mRNA binding proteins), allowing the cell to tightly regulated induction of other cytokines.[29] Many proinflammatory cytokines, especially

TNF-α, have unstable mRNAs, often because of the presence of cis-acting AREs in the 3′UTR which promote degradation.[30] Trans-acting factors including RBPs bind the AREs and regulate mRNA fate. HuR has been shown to recognize and bind the AREs of many cytokine transcripts, including TNF-α,[30,31] and seems to be the only identified RBP confirmed to stabilize, rather than destabilize, TNF-α transcripts.

HuR expression is increased in neointimal hyperplasia,[32] and induces VSMC constriction.[33] One report suggests that HuR is targeted by IL-10.[34] This study showed that HuR is expressed in an endothelial cell, VSMC, and macrophage in atherosclerotic plaque. We have previously reported that IL-19 affects HuR activity in cultured human VSMC.[9] However, a role for HuR in the mediation of IL-19 antiatherosclerotic activity in vivo are lacking. The present study extends those reports and demonstrates that compared with control mice, the absence of IL-19 significantly increases HuR mRNA and protein abundance systemically, in the spleen, and locally in the aortic arch. Further, cultured BMDM and VSMC isolated from dKO mice demonstrate increased amounts of HuR protein relative to cells cultured from *Ldlr*$^{-/-}$ mice. It was important to determine how IL-19 modifies HuR abundance. HuR mRNA contains conserved and semi-conserved ARE in its 3′UTR and is reported to regulate its own mRNA stability in a feedback mechanism.[35] We used cultured BMDM and VSMC treated with actinomycin D to determine that the absence of IL-19 results in an increase in HuR mRNA stability in both cell types. Notably, treatment with IL-19 in dKO cells rescued the phenotype, significantly reducing HuR mRNA stability below knock out levels, which may explain the increased HuR protein abundance in spleen and aortic arch in dKO mice. A consistent increase in HuR levels over the 14-week course of our study may lead to greater stability of proinflammatory transcripts and thus, exacerbated inflammation and plaque formation. It is important to note that there were no differences in the stability of proliferating cell nuclear antigen mRNA, which lacks AREs in its 3′UTR. This further supports the notion that increased stability of TNF-α mRNA in dKO cells is because of ARE-dependent stabilization of transcripts by excess HuR.

One mechanism of miRNA function is a reduction of mRNA abundance and subsequent reduction in protein. Stimulation with IL-19 induces expression of miRNA133a, a muscle cell-specific miRNA.[36] miR133a is predicted to target HuR 3′UTR, and this study showed that miR133a could reduce HuR mRNA and protein abundance. Importantly, miR133a expression was barely detectible in dKO VSMC but could be rescued to *Ldlr*$^{-/-}$ control levels with the addition of IL-19, providing a potential mechanism for IL-19 reduction of HuR. This may also explain the increased IL-19 sensitivity of VSMC compared with BMDM in terms of reduction of HuR mRNA stability (Figure 6D). One limitation of this study is that we cannot experimentally determine whether mRNA stability is modified in dKO mice because RNA transcription inhibitors including actinomycin D are toxic and cannot be used in vivo. However, considering the well-documented role of HuR as an mRNA stability protein together with its increased expression in spleen, aortic arch, and cells explanted from dKO mice, we feel confident that one major mechanism for IL-19 mediated atheroprotective effects is its ability to decrease HuR mRNA abundance, leading to decreases in mRNA stability of proinflammatory cytokines.

The regulation of mRNA stability and translation are 2 levels of post-transcriptional regulation that permit cells to rapidly respond to inflammatory stimuli.[31] Although modulation of mRNA stability has been posited as a possible therapeutic strategy,[37] surprisingly, there is very little literature exploring the concept of RBPs and mRNA stability being directly regulated by inflammatory stimuli. In conclusion, this article demonstrates that lack of IL-19 leads to increased atherosclerosis. This is likely because of increased mRNA stability of proinflammatory cytokines because of increased abundance of the mRNA stability protein, HuR. In the larger picture, it suggests that RBPs may represent a novel class of targets for modalities to attenuate vascular inflammation.

Acknowledgments

We would like to acknowledge the technical expertise of Lauren R. Beckett and Toby P. Thomas in performing these studies.

Sources of Funding

This study was supported by grants HL141108 and HL117724 from the National Heart, Lung, and Blood Institute of the National Institutes of Health, and grant 13GRNT1685003 from the American Heart Association to M.V. Autieri. M. Ray and A.B. Herman were supported by American Heart Association predoctoral fellowships 16PRE31220005 and 17PRE33670798, and grant 1F31HL137344-01 to A.B. Herman.

Disclosures

None.

References

1. Ross R. Atherosclerosis–an inflammatory disease. *N Engl J Med*. 1999;340:115–126. doi: 10.1056/NEJM199901143400207.
2. Libby P. Inflammation in atherosclerosis. *Nature*. 2002;420:868–874. doi: 10.1038/nature01323.
3. von der Thüsen JH, Kuiper J, van Berkel TJ, Biessen EA. Interleukins in atherosclerosis: molecular pathways and therapeutic potential. *Pharmacol Rev*. 2003;55:133–166. doi: 10.1124/pr.55.1.5.
4. Gabunia K, Jain S, England RN, Autieri MV. Anti-inflammatory cytokine interleukin-19 inhibits smooth muscle cell migration and activation of cytoskeletal regulators of VSMC motility. *Am J Physiol Cell Physiol*. 2011;300:C896–C906. doi: 10.1152/ajpcell.00439.2010.
5. Tian Y, Sommerville LJ, Cuneo A, Kelemen SE, Autieri MV. Expression and suppressive effects of interleukin-19 on vascular smooth muscle cell pathophysiology and development of intimal hyperplasia. *Am J Pathol*. 2008;173:901–909. doi: 10.2353/ajpath.2008.080163.
6. Ellison S, Gabunia K, Richards JM, Kelemen SE, England RN, Rudic D, Azuma YT, Munroy MA, Eguchi S, Autieri MV. IL-19 reduces ligation-mediated neointimal hyperplasia by reducing vascular smooth muscle cell activation. *Am J Pathol*. 2014;184:2134–2143. doi: 10.1016/j.ajpath.2014.04.001.
7. Oral HB, Kotenko SV, Yilmaz M, Mani O, Zumkehr J, Blaser K, Akdis CA, Akdis M. Regulation of T cells and cytokines by the interleukin-10 (IL-10)-family cytokines IL-19, IL-20, IL-22, IL-24 and IL-26. *Eur J Immunol*. 2006;36:380–388. doi: 10.1002/eji.200425523.
8. Gallagher G, Dickensheets H, Eskdale J, Izotova LS, Mirochnitchenko OV, Peat JD, Vazquez N, Pestka S, Donnelly RP, Kotenko SV. Cloning, expression and initial characterization of interleukin-19 (IL-19), a novel homologue of human interleukin-10 (IL-10). *Genes Immun*. 2000;1:442–450. doi: 10.1038/sj.gene.6363714.
9. Cuneo AA, Herrick D, Autieri MV. Il-19 reduces VSMC activation by regulation of mRNA regulatory factor HuR and reduction of mRNA stability. *J Mol Cell Cardiol*. 2010;49:647–654. doi: 10.1016/j.yjmcc.2010.04.016.
10. Ellison S, Gabunia K, Kelemen SE, England RN, Scalia R, Richards JM, Orr AW, Orr W, Traylor JG Jr, Rogers T, Cornwell W, Berglund LM,

Goncalves I, Gomez MF, Autieri MV. Attenuation of experimental atherosclerosis by interleukin-19. *Arterioscler Thromb Vasc Biol*. 2013;33:2316–2324. doi: 10.1161/ATVBAHA.113.301521.
11. Gabunia K, Ellison S, Kelemen S, Kako F, Cornwell WD, Rogers TJ, Datta PK, Ouimet M, Moore KJ, Autieri MV. IL-19 halts progression of atherosclerotic plaque, polarizes, and increases cholesterol uptake and efflux in macrophages. *Am J Pathol*. 2016;186:1361–1374. doi: 10.1016/j.ajpath.2015.12.023.
12. England RN, Preston KJ, Scalia R, Autieri MV. Interleukin-19 decreases leukocyte-endothelial cell interactions by reduction in endothelial cell adhesion molecule mRNA stability. *Am J Physiol Cell Physiol*. 2013;305:C255–C265. doi: 10.1152/ajpcell.00069.2013.
13. Sommerville LJ, Kelemen SE, Ellison SP, England RN, Autieri MV. Increased atherosclerosis and vascular smooth muscle cell activation in AIF-1 transgenic mice fed a high-fat diet. *Atherosclerosis*. 2012;220:45–52. doi: 10.1016/j.atherosclerosis.2011.07.095.
14. Hansson GK, Libby P. The immune response in atherosclerosis: a double-edged sword. *Nat Rev Immunol*. 2006;6:508–519. doi: 10.1038/nri1882.
15. Fan XC, Steitz JA. Overexpression of HuR, a nuclear-cytoplasmic shuttling protein, increases the in vivo stability of ARE-containing mRNAs. *EMBO J*. 1998;17:3448–3460. doi: 10.1093/emboj/17.12.3448.
16. Schoenberg DR, Maquat LE. Regulation of cytoplasmic mRNA decay. *Nat Rev Genet*. 2012;13:246–259. doi: 10.1038/nrg3160.
17. Gabunia K, Herman AB, Ray M, Kelemen SE, England RN, DeLa Cadena R, Foster WJ, Elliott KJ, Eguchi S, Autieri MV. Induction of MiR133a expression by IL-19 targets LDLRAP1 and reduces oxLDL uptake in VSMC. *J Mol Cell Cardiol*. 2017;105:38–48. doi: 10.1016/j.yjmcc.2017.02.005.
18. Schulte S, Sukhova GK, Libby P. Genetically programmed biases in Th1 and Th2 immune responses modulate atherogenesis. *Am J Pathol*. 2008;172:1500–1508. doi: 10.2353/ajpath.2008.070776.
19. Mallat Z, Ait-Oufella H, Tedgui A. Regulatory T cell responses: potential role in the control of atherosclerosis. *Curr Opin Lipidol*. 2005;16:518–524.
20. Frostegård J, Ulfgren AK, Nyberg P, Hedin U, Swedenborg J, Andersson U, Hansson GK. Cytokine expression in advanced human atherosclerotic plaques: dominance of pro-inflammatory (Th1) and macrophage-stimulating cytokines. *Atherosclerosis*. 1999;145:33–43.
21. Potteaux S, Esposito B, van Oostrom O, Brun V, Ardouin P, Groux H, Tedgui A, Mallat Z. Leukocyte-derived interleukin 10 is required for protection against atherosclerosis in low-density lipoprotein receptor knockout mice. *Arterioscler Thromb Vasc Biol*. 2004;24:1474–1478. doi: 10.1161/01.ATV.0000134378.86443.cd.
22. Caligiuri G, Rudling M, Ollivier V, Jacob MP, Michel JB, Hansson GK, Nicoletti A. Interleukin-10 deficiency increases atherosclerosis, thrombosis, and low-density lipoproteins in apolipoprotein E knockout mice. *Mol Med*. 2003;9:10–17.
23. Mallat Z, Besnard S, Duriez M, Deleuze V, Emmanuel F, Bureau MF, Soubrier F, Esposito B, Duez H, Fievet C, Staels B, Duverger N, Scherman D, Tedgui A. Protective role of interleukin-10 in atherosclerosis. *Circ Res*. 1999;85:e17–e24.
24. Tedgui A, Mallat Z. Cytokines in atherosclerosis: pathogenic and regulatory pathways. *Physiol Rev*. 2006;86:515–581. doi: 10.1152/physrev.00024.2005.
25. Gallagher G, Eskdale J, Jordan W, Peat J, Campbell J, Boniotto M, Lennon GP, Dickensheets H, Donnelly RP. Human interleukin-19 and its receptor: a potential role in the induction of Th2 responses. *Int Immunopharmacol*. 2004;4:615–626. doi: 10.1016/j.intimp.2004.01.005.
26. Gallagher G. Interleukin-19: multiple roles in immune regulation and disease. *Cytokine Growth Factor Rev*. 2010;21:345–352. doi: 10.1016/j.cytogfr.2010.08.005.
27. Wegenka UM. IL-20: biological functions mediated through two types of receptor complexes. *Cytokine Growth Factor Rev*. 2010;21:353–363. doi: 10.1016/j.cytogfr.2010.08.001.
28. Yeh CH, Cheng BC, Hsu CC, Chen HW, Wang JJ, Chang MS, Hsing CH. Induced interleukin-19 contributes to cell-mediated immunosuppression in patients undergoing coronary artery bypass grafting with cardiopulmonary bypass. *Ann Thorac Surg*. 2011;92:1252–1259. doi: 10.1016/j.athoracsur.2011.04.061.
29. Anderson P. Post-transcriptional control of cytokine production. *Nat Immunol*. 2008;9:353–359. doi: 10.1038/ni1584.
30. Khera TK, Dick AD, Nicholson LB. Mechanisms of TNFα regulation in uveitis: focus on RNA-binding proteins. *Prog Retin Eye Res*. 2010;29:610–621. doi: 10.1016/j.preteyeres.2010.08.003.
31. Palanisamy V, Jakymiw A, Van Tubergen EA, D'Silva NJ, Kirkwood KL. Control of cytokine mRNA expression by RNA-binding proteins and microRNAs. *J Dent Res*. 2012;91:651–658. doi: 10.1177/0022034512437372.
32. Pullmann R Jr, Juhaszova M, López de Silanes I, Kawai T, Mazan-Mamczarz K, Halushka MK, Gorospe M. Enhanced proliferation of cultured human vascular smooth muscle cells linked to increased function of RNA-binding protein HuR. *J Biol Chem*. 2005;280:22819–22826. doi: 10.1074/jbc.M501106200.
33. Pende A, Contini L, Sallo R, Passalacqua M, Tanveer R, Port JD, Lotti G. Characterization of RNA-binding proteins possibly involved in modulating human AT 1 receptor mRNA stability. *Cell Biochem Funct*. 2008;26:493–501. doi: 10.1002/cbf.1472.
34. Rajasingh J, Bord E, Luedemann C, Asai J, Hamada H, Thorne T, Qin G, Goukassian D, Zhu Y, Losordo DW, Kishore R. IL-10-induced TNF-alpha mRNA destabilization is mediated via IL-10 suppression of p38 MAP kinase activation and inhibition of HuR expression. *FASEB J*. 2006;20:2112–2114. doi: 10.1096/fj.06-6084fje.
35. Dai W, Zhang G, Makeyev EV. RNA-binding protein HuR autoregulates its expression by promoting alternative polyadenylation site usage. *Nucleic Acids Res*. 2012;40:787–800. doi: 10.1093/nar/gkr783.
36. Williams AH, Liu N, van Rooij E, Olson EN. MicroRNA control of muscle development and disease. *Curr Opin Cell Biol*. 2009;21:461–469. doi: 10.1016/j.ceb.2009.01.029.
37. Eberhardt W, Doller A, Akool el-S, Pfeilschifter J. Modulation of mRNA stability as a novel therapeutic approach. *Pharmacol Ther*. 2007;114:56–73. doi: 10.1016/j.pharmthera.2007.01.002.

Highlights

- *Il19*$^{-/-}$×*Ldlr*$^{-/-}$ double knockout mice have significantly more atherosclerotic plaque compared with *Ldlr*$^{-/-}$ controls.
- Double knockout mice have increased proinflammatory cytokine expression in aorta and spleen and increased proinflammatory cytokine expression and mRNA stability in bone marrow-derived macrophages and vascular smooth muscle cells.
- Double knockout mice have increased expression of the mRNA stability protein HuR (human antigen R) in aorta, spleen and increased expression and mRNA stability of HuR in bone marrow-derived macrophage and vascular smooth muscle cell.
- All of the above phenotypes can be rescued by the addition of mouse IL (interleukin)-19 in vivo and in vitro.
- These data indicate that IL-19 is an atheroprotective cytokine that decreases the abundance of HuR, leading to reduced proinflammatory mRNA stability.

Arteriosclerosis, Thrombosis, and Vascular Biology

Journal of the American Heart Association

Genetic Deletion of IL (Interleukin)-19 Exacerbates Atherogenesis in *Il19*$^{-/-}$×*Ldlr*$^{-/-}$ Double Knockout Mice by Dysregulation of mRNA Stability Protein HuR (Human antigen R)

Mitali Ray, Khatuna Gabunia, Christine N. Vrakas, Allison B. Herman, Farah Kako, Sheri E. Kelemen, Laurel A. Grisanti and Michael V. Autieri

Arterioscler Thromb Vasc Biol. published online April 19, 2018;
Arteriosclerosis, Thrombosis, and Vascular Biology is published by the American Heart Association, 7272 Greenville Avenue, Dallas, TX 75231

Print ISSN: 1079-5642. Online ISSN: 1524-4636

Materials and Methods A detailed listing of mice and antibodies used are listed in the jajor resouce table in the Supplementary Material section.

RNA extraction and quantitative RT-PCR. RNA from spleen, aortic arch, and cultured cells was isolated using the RNeasy PowerLyzer Tissue & Cells Kit (Qiagen) and Direct-zol™ RNA Miniprep Plus (Zymo Research) for tissue and cells, respectively, according to the manufacturer's protocol. 200ng of RNA from each sample was reverse transcribed using Maxima First Strand cDNA Synthesis kit for qRT-PCR (Thermo Scientific) as previously described, and target genes were amplified using SYBR green (Thermo Scientific) and gene-specific primers, in triplicate, using an Eppendorf Realplex4 Mastercycler[6,9-12]. Ct values were quantitated by the Eppendorf software. Results were normalized using the housekeeping gene GAPDH or β-2 Microglobulin and relative gene expression was calculated and graphed as fold change ($2^{-\Delta\Delta Ct}$) from control. Primer pairs were purchased from Integrated DNA Technologies. The following primer pairs were used:
Arginase1: F- 5'AAGAATGGAAGAGTCAGTGTGG3', R- 5'GGGAGTGTTGATGTCAGTGTG3';
Arginase 2: F- 5'CAGAAGGTGATGGAACAGACA3', R- 5'GCCAGTTTAGGGTCAAATGC3';
β-2 Microglobulin: F- 5'ATGTGAGGCGGGTGGAACTG3', R- CTCGGTGACCCTGGTCTTTCTG3';
FOXP3: F- 5'AAGTACCACAATATGCGACCC3', R- 5'TCTGAAGTAGGCGAACATGC3';
GAPDH: F- 5'GCAAGGACACTGAGCAAGAG3', R- 5'GGGTCTGGGATGGAAATTGT3';
GATA3: F- 5'TACCACCTATCCGCCCTATG3', R- 5'CTCGACTTACATCCGAACCC3';
HuR: F- 5'GGGATAAAGTAGCAGGACACAG3', R- 5'TTGGGCGAGCATATGACAC3';
IL-1β: F- 5'CTAATAGGCTCATCTGGGATCC3', R- 5'GGTCCGTCAACTTCAAAGAAC3';
IL-10: F- 5'CTGTGTTTAAGCTGTTTCCATTGG3', R- 5'AGGAAGAACCCCTCCCATCAT3';
IL-12β: F- 5'GTGAAGCACCAAATTACTCCG3', R- 5'AGAGACGCCATTCCACATG3';
iNOS: F- 5'TTTGACGCTCGGAACTGTAG3', R- 5'GAGCCTGAAGTCATGTTTGC3';
MCP1: F- 5'TTAAAAACCTGGATCGGAACCAA3', R- 5'GCATTAGCTTCAGATTTACGGGT3';
PCNA: F- 5'GGGTGAAGTTTTCTGCAAGTG3', R- 5'GTACCTCAGAGCAAACGTTAGG3';
RORγ: F- 5'TTTCTGAGGATGAGATTGCCC3', R- 5'TTGTCGATGAGTCTTGCAGAG3';
T-Bet: F- 5'CCTGTTGTGGTCCAAGTTCAAC3', R- 5'CACAAACATCCTGTAATGGCTTGT3';
TNFα: F- 5'CTTCTGTCTACTGAACTTCGGG3', R- 5'CAGGCTTGTCACTCGAATTTTG3'
miR133a levels were detected using miScript II RT Kit, miScript SYBR Green PCR Kit, and miScript Primer Assay (Qiagen).

Western blotting. Protein extracts made as described were separated by SDS-PAGE, transferred to nitrocellulose membrane, incubated with a 1:3000 dilution of primary antibody HuR or TNFα (abcam, Santa Cruz Biotechnology), followed by a 1:4000 dilution of secondary antibody[4,9-12]. Equal loading of protein extracts on gels was verified by Ponceau S staining of the membrane, and blotting with the housekeeping protein anti-GAPDH or HSC70 (Cell Signaling Technology, Santa Cruz Biotechnology), and reactive proteins were visualized using enhanced chemiluminescence. The intensity of each band was quantitated using image analysis software (NIH Image J).

Immunohistochemistry. Aortic roots were frozen in OCT and 5 µm-thick serial sections were cut and placed on microscope slides. Immunoperoxidase staining (see below) was performed using CD68 antibody (Biolegend). Positively stained areas (brown) were quantified as a percentage of total lesion areas by quantitative morphometry, using 4 sections per aortic root, as described previously by us and others[9-12,37]. Aortas from *Ldlr*$^{-/-}$ mice on high fat diet for 14 weeks and from

C57BL/6 wild type mice on a normal diet were removed, formalin fixed and paraffin embedded (FFPE), and cut into 5 µm-thick sections. For immunoperoxidase staining for HuR, sections were deparaffinized and heat mediated antigen unmasking (Vector Labs) was performed. Sections were blocked with 5% goat serum (Vector) for 30 minutes, incubated with HuR (Abcam) primary antibody for 2 hours, washed, and incubated with secondary antibody conjugated to Biotin (Vector Labs) for 30 minutes. This was followed by Avitin-Biotin-Horseradish peroxidase complex and diaminobenzidine (DAB) substrate (brown stain) (Vector Labs Inc.) and counterstained with hematoxylin (blue stain). Immunofluorescent staining was performed on the same aortas (FFPE) mentioned above. Staining protocol is essentially identical to immunoperoxidase staining except that: tissues were blocked with 5% donkey serum (Jackson ImmunoResearch Labs, Inc.) for 30 mins., and the secondary antibodies are conjugated to fluorescent tags. HuR was visualized by using a donkey anti-rabbit secondary antibody conjugated to Alexafluor 568 (red), smooth muscle cell α actin, CD31, and CD68 were all visualized by using a secondary antibody conjugated to Alexafluor 488 (green) (Jackson ImmunoResearch Labs, Inc). Images were captured with an Olympus BX40 microscope and analyzed using Image J.

Intracellular Staining and Flow Cytometry. Flow cytometry analysis was performed on whole blood from mice to detect TNFα in peripheral blood lymphocytes. Briefly, red blood cells were lysed using lysing buffer (BD Pharm Lyse), leukocytes were cultured in RPMI 1640 medium supplemented with 10% FBS and stimulated with cell stimulation cocktail (eBioscience, Catalog #00-4975) for 5 hours. $1x10^6$ cells were harvested, washed in flow cytometry staining buffer (eBioscience, Catalog #00-4222), surface stained with Qdot605 conjugated anti-mouse CD4 (clone RM4-5) antibody, fixed and permeabilized using the Cytofix/Cytoperm Kit (BD Pharmingen) according to manufacturer's instructions. For intracellular staining, cells were incubated with either APC-conjugated anti-mouse TNFα antibody (clone MP6-XT22) or its isotype control Rat IgG1κ (eBRG1) (eBioscience). Acquisition was performed on LSR II flow cytometer with FACSDiva software (BD Biosciences), and data was analyzed with FlowJo software (Tree Star).

For identification of cell subsets within whole blood for complete blood counts, blood was collected retro-orbitally using heparinized capillary tubes, diluted with 3.8% sodium citrate, and analyzed using morphological flagging by Hemavet 950S analyzer (Drew Scientific).

Statistical analysis. Results are expressed as mean ± SEM. Differences between groups were evaluated with the use of ANOVA, with the Newman-Keuls method applied to evaluate differences between individual mean values or by unpaired Student's *t* test and a *p* value of <0.05 was considered indicative of a statistically significant result. D'Agostino's K^2 and F tests were performed to confirm data passed normality and equal variance for Student's *t* tests.

Major Resources Tables

Animals

Species/Strain	Vendor or Source	Background Strain	Sex
Ldlr$^{-/-}$ mouse	Jackson Labs	C57BL/6	M, F
Il19$^{-/-}$ x *Ldlr*-/- mouse	generated in house	C57BL/6	M, F

Antibodies

Target antigen	Vendor or Source	Catalog #	Working concentration	Lot # (preferred but not required)
HuR	abcam	200342	1:3000	
TNFα	Santa Cruz Biotechnology	SC-52746	1:3000	E0813
GAPDH	Cell Signaling Technology	14C10	1:3000	
HSC70	Santa Cruz Biotechnology	SC-7298	1:3000	I032

Supplement Material

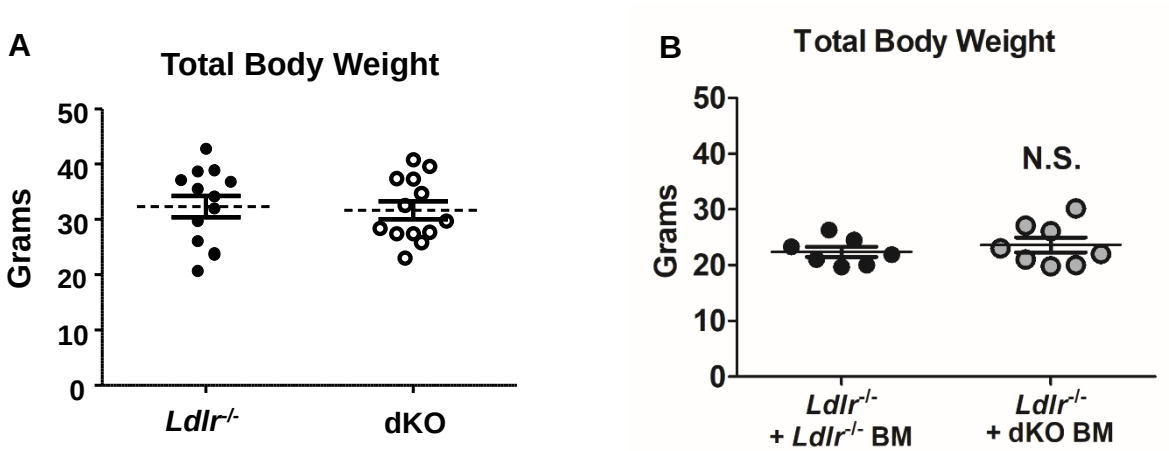

Supplemental Data Figure I. A All *Ldlr*$^{-/-}$ and dKO mice do not statistically differ in total weight after 14 weeks of HFD feeding; no differences were found across sex (32.21 ± 1.92g in *Ldlr*$^{-/-}$ vs 31.67 ± 1.56g in dKO; *n*=12 *Ldlr*$^{-/-}$ vs 13 dKO).
B *Ldlr*$^{-/-}$ mouse recipients of dKO bone marrow (BM) do not differ from recipients of *Ldlr*$^{-/-}$ BM in total body weight following 14 weeks of HFD; no differences were found across sex (22.39 ± 0.92g in *Ldlr*$^{-/-}$ recipients vs 23.65 ± 1.67g in dKO recipients; *n*=7 *Ldlr*$^{-/-}$ recipients vs 8 dKO recipients)**.**

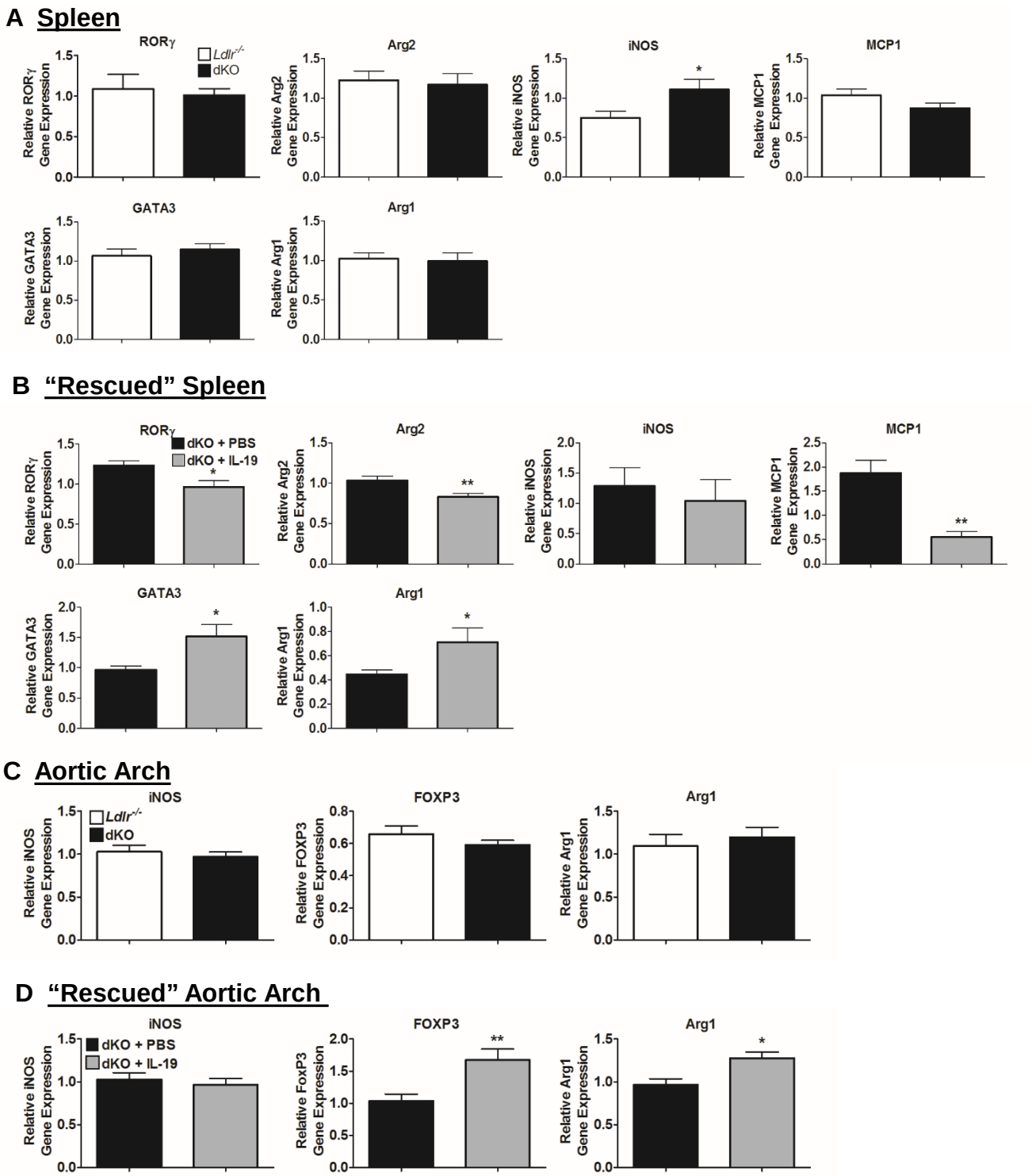

Supplemental Data Figure II.
Additional quantitative RT-PCR analysis of spleen and aortic arch harvested from *Ldlr*$^{-/-}$ and dKO mice after 14 weeks of HFD (**A**, **C**) and dKO mice simultaneously injected with IL-19 or PBS during HFD feeding (**B**, **D**). At the time of euthanasia. RNA was extracted, reverse transcribed, and amplified using primers for the genes shown. (*n*=8 spleen, aortic arch per group).

A Flow Cytometry

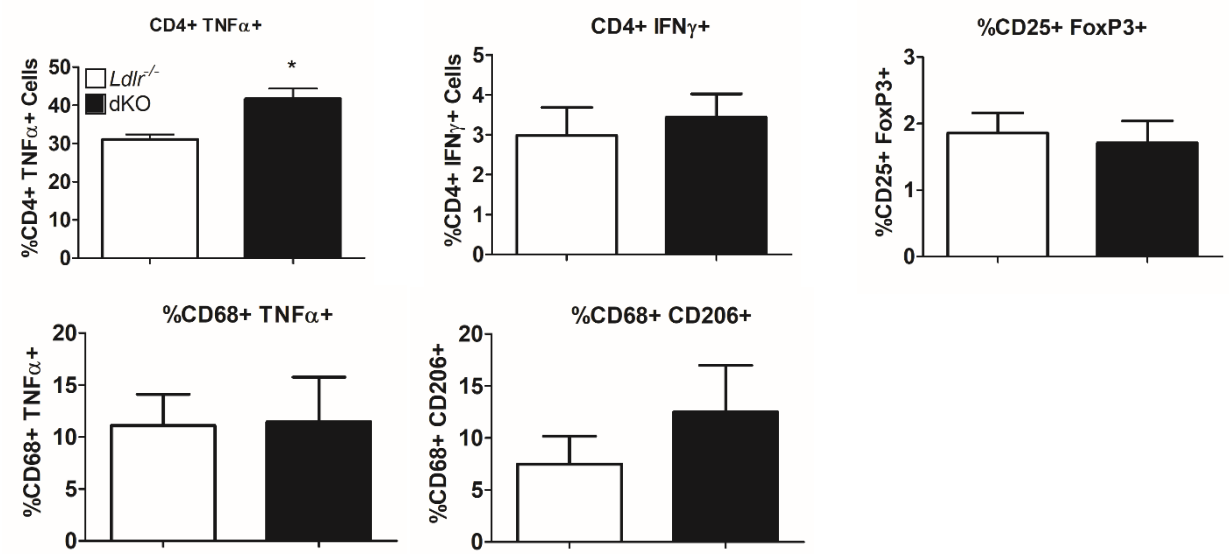

B Blood Count

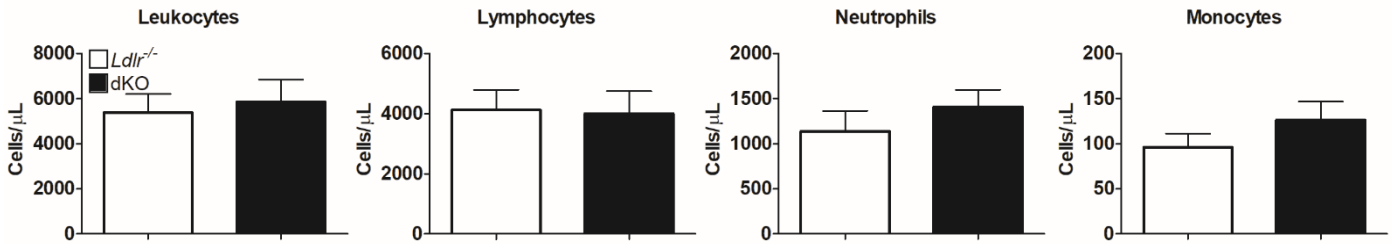

C Bone Marrow Transplant Blood Count

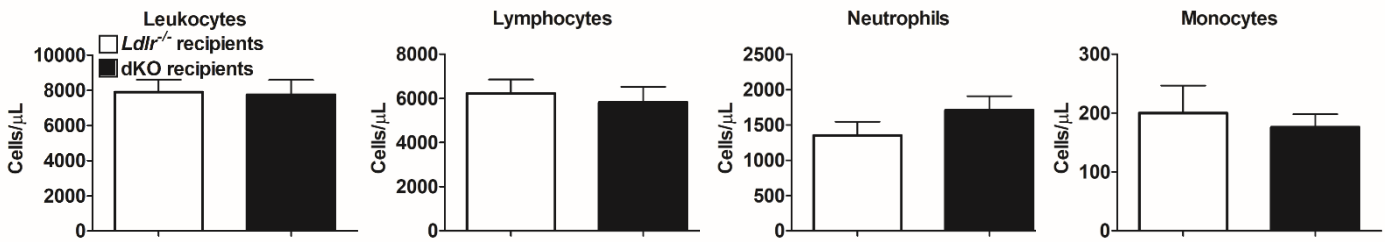

Supplemental Data Figure III Effects of deletion of IL-19 in circulating immune cells. Circulating cells were quantitated by flow cytometry (**A**) and complete blood count was analyzed by Hemavet (**B**) from peripheral blood obtained from *Ldlr*$^{-/-}$ and dKO mice after 14 weeks of HFD consumption, at the time of euthanasia. DKO mice had a significantly higher percentage of CD4+ TNFα+ T cells compared to control mice (*n*=4 per group).

C Complete blood counts from *Ldlr*$^{-/-}$ mice that were recipients of dKO BM did not differ from recipients of *Ldlr*$^{-/-}$ BM (*n*=7 *Ldlr*$^{-/-}$ recipients vs 8 dKO recipients)

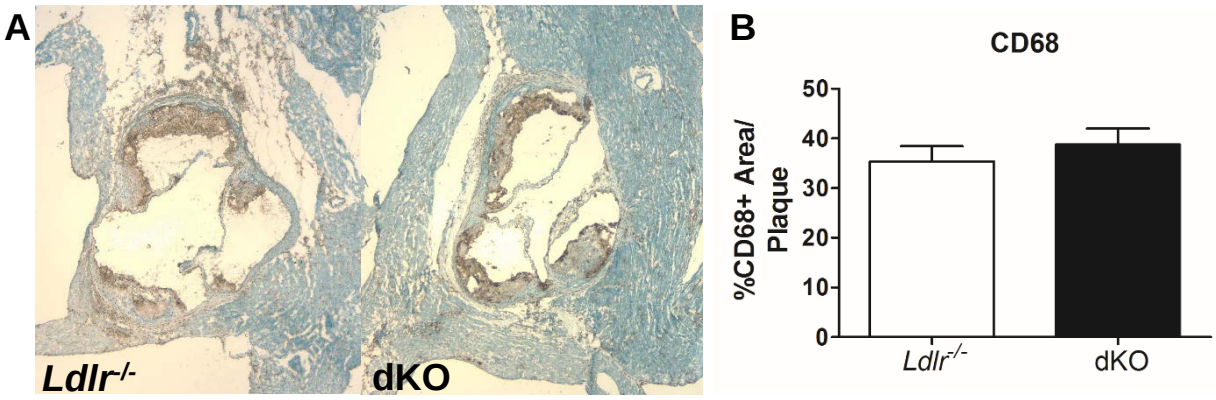

Supplemental Data Figure IV. Loss of IL-19 does not affect macrophage infiltrate in atherosclerotic lesions. **A** Aortic roots were harvested from *Ldlr*$^{-/-}$ and dKO mice after 14 weeks of HFD. Multiple serial sections of aortic root from the aortic sinus to the disappearance of valve cusps per root from were from sectioned and immunostained using anti-CD68 antibody. **B** Positively stained areas were quantified as a percentage of total lesion areas by quantitative morphometry. (35.38 ± 3.06% in *Ldlr*$^{-/-}$ vs 38.75 ± 3.27% in dKO, *n*=6 per group).

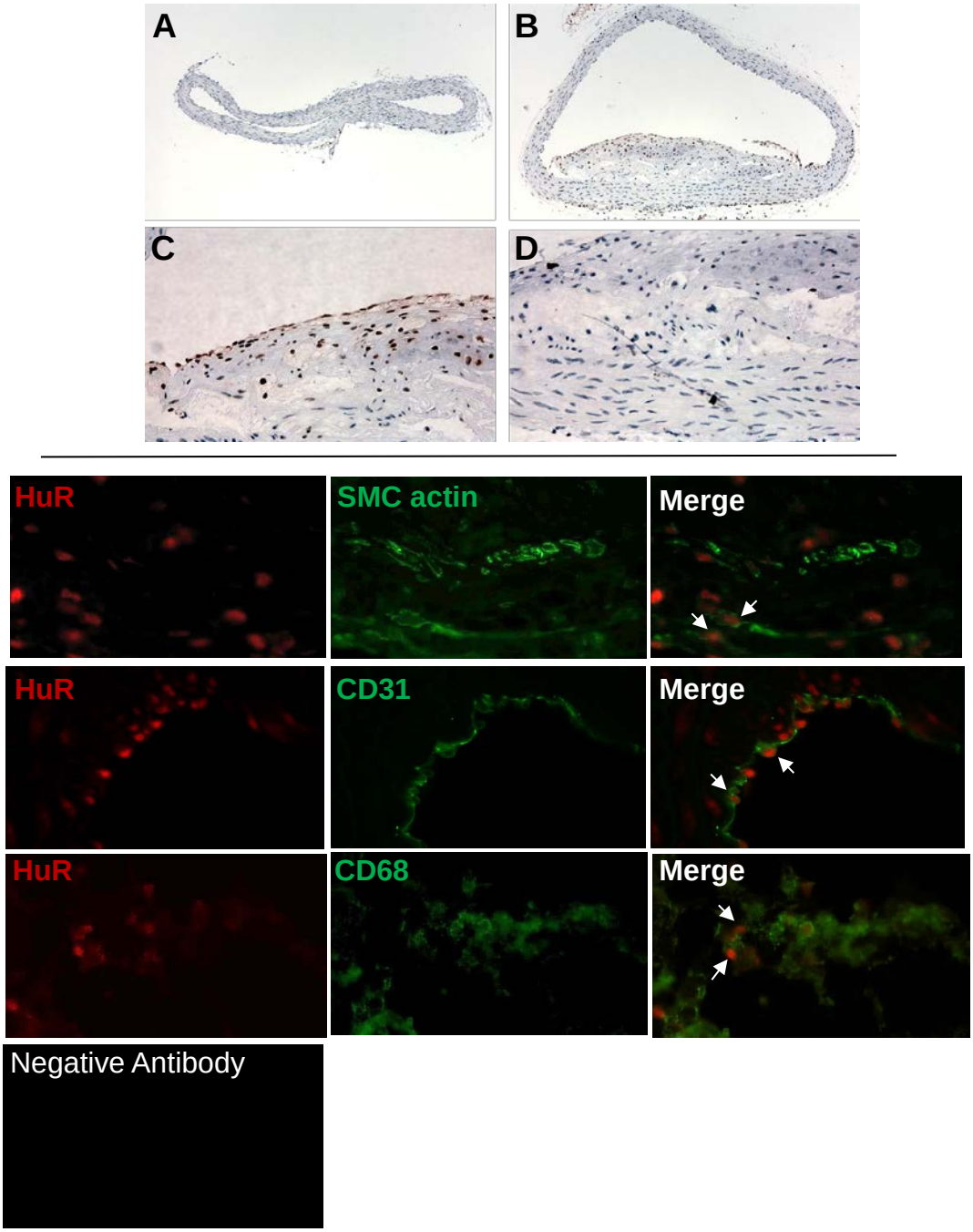

Supplemental Data Figure V. Expression of HuR in atherosclerotic plaque.
Top: Immunohistochemistry on mouse aortas. Expression of HuR is brown and hematoxylin counterstain in blue. **A** There is no expression of HuR in healthy C57BL/6 wild type aorta.
B Expression of HuR is present in the atherosclerotic plaque of an aorta from an *Ldlr*$^{-/-}$ mouse fed high fat diet for 14 weeks; 400X shown in **C**. **D** Same tissue as B and C with negative control antibody.
Bottom: In the same atherosclerotic plaque of an aorta from a *Ldlr*$^{-/-}$ mouse fed high fat diet for 14 weeks, expression of HuR was seen in smooth muscle cells (SMCactin), endothelial cells (CD31) and macrophages (CD68) by immunofluorescent co-localization staining (arrows indicate co-localization). Isotype negative control antibodies were used for each type of antibody. Magnification 600X.

A

```
Position 673-680 of ELAVL1 3' UTR  5'  ...GGCACCAAUGGGAAUGGACCAAA...
                                                    |||||||        8mer
hsa-miR-133a                       3'     GUCGACCAACUUCCCCUGGUUU
```

B **Aortic Arch**

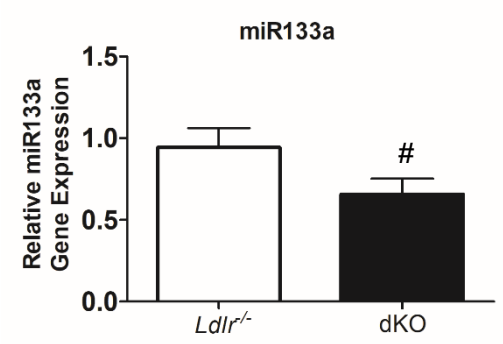

Supplemental data Figure VI. **A** Predicted consequential pairing of target region (top) and miRNA133a (bottom). Targetscan analysis identifies seed regions of miR133a which target regions of HuR 3'UTR mRNA. The locations of the miR133a complementary sites on human HuR 3′UTR are shown.

B qRT-PCR analysis from aortic arch from *Ldlr*$^{-/-}$ and dKO mice after 14 weeks of HFD feeding shows insignificantly decreased levels of miR133a in dKO (# indicates p=0.074)

Spleen			
Gene	**Fold Change**		***p* value**
	Ldlr$^{-/-}$	**dKO**	
TNFα	1.160 ± 0.185	2.007 ± 0.203	<0.01
TBet	0.566 ± 0.136	2.527 ± 0.341	<0.001
IL-12β	1.909 ± 0.541	4.676 ± 0.889	<0.05
IL-1β	1.340 ± 0.330	3.205 ± 0.268	<0.001
FOXP3	1.188 ± 0.201	0.607 ± 0.073	<0.05
IL-10	1.049 ± 0.095	0.436 ± 0.120	<0.001
RORγ	1.090 ± 0.176	1.010 ± 0.082	N.S.
Arg2	1.228 ± 0.114	1.168 ± 0.143	N.S.
iNOS	0.749 ± 0.087	1.108 ± 0.087	<0.05
MCP1	1.034 ± 0.079	0.871 ± 0.064	N.S.
GATA3	1.065 ± 0.085	1.146 ± 0.074	N.S.
Arg1	1.022 ± 0.077	0.990 ± 0.108	N.S.
"Rescued" Spleen			
Gene	**Fold Change**		***p* value**
	dKO + PBS	**dKO + IL-19**	
TNFα	2.497 ± 0.169	0.988 ± 0.176	<0.001
TBet	3.234 ± 0.349	1.889 ± 0.286	<0.01
IL-12β	2.060 ± 0.523	0.685 ± 0.184	<0.05
IL-1β	2.469 ± 0.210	0.578 ± 0.139	<0.001
FOXP3	0.596 ± 0.069	1.277 ± 0.066	<0.001
IL-10	0.998 ± 0.246	4.119 ± 0.573	<0.001
RORγ	1.234 ± 0.058	0.966 ± 0.078	<0.05
Arg2	1.032 ± 0.054	0.830 ± 0.043	<0.01
iNOS	1.282 ± 0.303	1.041 ± 0.348	N.S.
MCP1	1.878 ± 0.267	0.554 ± 0.110	<0.01
GATA3	0.964 ± 0.061	1.520 ± 0.199	<0.05
Arg1	0.446 ± 0.037	0.710 ± 0.119	<0.05

Supplemental Table I. qRT-PCR fold change and *p* values.
Fold change ($2^{-\Delta\Delta CT}$) and *p* values for various genes from quantitative RT-PCR analysis of spleen harvested from *Ldlr$^{-/-}$* and dKO mice after 14 weeks of HFD and dKO mice simultaneously injected with IL-19 or PBS during HFD feeding.
Data shown graphically in Figures 2A, 2B and Supplemental Data Figures IIA, IIB.

Aortic Arch			
Gene	**Fold Change**		***p* value**
	Ldlr$^{-/-}$	**dKO**	
TNFα	1.006 ± 0.033	1.263 ± 0.033	<0.001
TBet	0.243 ± 0.109	0.756 ± 0.054	<0.001
Arg2	1.846 ± 0.348	2.926 ± 0.273	<0.001
IL-12β	1.375 ± 0.382	3.088 ± 0.552	<0.05
IL-1β	0.879 ± 0.219	1.645 ± 0.244	<0.05
MCP1	0.802 ± 0.070	1.030 ± 0.076	<0.001
RORγ	1.147 ± 0.197	2.608 ± 0.265	<0.001
GATA3	0.375 ± 0.058	0.181 ± 0.017	<0.01
IL-10	0.767 ± 0.047	0.589 ± 0.046	<0.01
iNOS	1.028 ± 0.073	0.967 ± 0.073	N.S.
FOXP3	0.657 ± 0.052	0.591 ± 0.028	N.S.
Arg1	1.022 ± 0.077	0.990 ± 0.108	N.S.
"Rescued" Aortic Arch			
Gene	**Fold Change**		***p* value**
	dKO + PBS	**dKO + IL-19**	
TNFα	1.115 ± 0.038	0.861 ± 0.012	<0.001
TBet	2.327 ± 0.500	0.880 ± 0.163	<0.01
Arg2	1.184 ± 0.038	0.794 ± 0.141	<0.05
IL-12β	1.392 ± 0.101	0.967 ± 0.073	<0.01
IL-1β	1.479 ± 0.062	0.863 ± 0.030	<0.001
MCP1	1.376 ± 0.319	0.566 ± 0.095	<0.05
RORγ	1.216 ± 0.258	0.616 ± 0.080	<0.05
GATA3	1.216 ± 0.258	0.616 ± 0.080	<0.05
IL-10	1.017 ± 0.065	1.376 ± 0.059	<0.001
iNOS	1.027 ± 0.082	0.966 ± 0.073	N.S.
FOXP3	1.033 ± 0.110	1.668 ± 0.171	<0.01
Arg1	0.963 ± 0.072	1.272 ± 0.076	<0.05

Supplemental Table II. qRT-PCR fold change and *p* values. Fold change ($2^{-\Delta\Delta CT}$) and *p* values for various genes from quantitative RT-PCR analysis of aortic arch harvested from *Ldlr$^{-/-}$* and dKO mice after 14 weeks of HFD and dKO mice simultaneously injected with IL-19 or PBS during HFD feeding. Data shown graphically in Figures 2A, 2B and Supplemental Data Figures IIA, IIB.